

SIMPLIFIED ANALYSIS OF ELECTRICAL GRADIENTS ABOVE A GROUND GRID - I
How Good Is The Present IEEE Method? (A Special Report For WG 78.1)

J. G. Sverak, Senior Member, IEEE
Gibbs & Hill, Inc.
New York, N. Y.

Abstract -- Referring to the 1976 edition of IEEE Std 80, this paper examines the basic premises of IEEE gradient method and of simplified equations for determining the touch and step voltages in the corner mesh of a grounding grid. Re-examination of the principal assumptions yields a new simplified formula for K_m which performs the calculation with less error. A beneficial effect of ground rods is evaluated in view of the present equation for the current irregularity factor K_i . A brief analysis of the effect of a crush-stone overlay upon the allowable surface voltage above and beyond a grounding grid, is also included. A review of work done by others related to the methods of Std 80 includes a discussion of equations and of some critical aspects involved. A computer-produced series, comparing the performance of the old simplified and non-simplified equations for K_m with the improved ones and with the equations suggested by Thapar and Nagar, Zukerman, Zink, and Nahman, concludes Part I of this two-part report. Its purpose is to provide a framework for updating and refining Appendix I of the Guide which is presently under revision.

1. INTRODUCTION

Two decades ago, a simple and reasonably accurate method for grounding calculations was thought to be at hand. In 1958, AIEE Substation Committee Report, prepared by a small working group led by Stevens, was published in the AIEE Transactions under the title "Voltage Gradients Through the Ground Under Fault Conditions". In 1961, this report became a core of the AIEE Guide 80, and consequently, of the IEEE Std. 80-1976. /1,2,3/

Using as a bench mark the result of measurements done by Koch on very small-scale models of square grids in an electrolytic tank, a remarkably simple method for determining the effects of a grid geometry upon the step and touch/mesh voltages was devised. The method centers on determining three major coefficients, K_m , K_s , and K_i , which are used in evaluating the step and touch voltages above a grounding grid, as follows:

$$E_{\text{mesh}} = \sigma K_m K_i I_o / L \quad \text{and} \quad E_{\text{step}} = \sigma K_s K_i I_o / L \quad (1),(2)$$

where σ is soil resistivity, in ohm-meters

K_m is mesh voltage factor

K_s is step voltage factor

K_i is current irregularity corrective factor

I_o is grid current, in amperes

L is total length of grid conductors + (optionally) total length of ground rods, in meters

While both K_m and K_s are reasonably simple functions of a number of parallel conductors N , their spacing D , diameter d , and depth of a grid burial h , i.e.

$$K_m = f(N,h,D,d) \quad \text{and} \quad K_s = f(N,h,D,d) \quad (3),(4)$$

the application of the third factor K_i , also called "current irregularity factor", has not been clearly defined. The designer is left to decide himself if a) to determine K_i as a simple linear function of N , specifically as

$$K_i = f(N) = 0.172 N + 0.65 \quad (5)$$

or b) use an arbitrary value, totally dependent on his judgement and experience, at best assisted by inspection of Figure 8, page 23 of the subject Guide, showing a few square grid patterns with so pre-calculated products of K_i and K_m , as to match the already mentioned Koch's experimental data, or c) select this value from a typical range of K_i values, given elsewhere in the Guide as 1.2 - 2 or "slightly more", without attempting to analyze the design further.

Nonetheless, despite minor reservations voiced by Schwarz in his discussion of the original AIEE report - mostly in regard to the general applicability of the "typical" values above - which he felt to be too low, the overall concept of this method has been enthusiastically received by the industry. In fact, according to the recent international survey, the Guide is regarded by many as the only reference book for grounding design which has been accepted practically world-wide. /4/

83 WM 104-7 A paper recommended and approved by the IEEE Substations Committee of the IEEE Power Engineering Society for presentation at the IEEE/PES 1983 Winter Meeting, New York, New York, January 30-February 4, 1983.

Manuscript submitted September 21, 1982;

made available for printing November 30, 1982.

In order to truly appreciate the method as a contribution to the art of grounding, one has to realize that in the early fifties, both the scarcity of computing facilities and the limited opportunity to use a computer systematically, hampered the chances to discover any computational anomaly or peculiarity of the method. Though some pioneering work on computer was done by Gross et al, their research concentrated more on an exact calculation of the ground resistances of rectangular grids and plates (an averaging problem), than on the effect of electric gradients above a grid, concerning extremities. /5/

However, soon in the following years, the validity of several assumptions became questioned. In the seventies, first Mukhedkar and Dawalibi, Sverak, and later Zukerman, Nahman and Skuletich, and Zink, have each dealt with some of the following problems, known to this date; references /6,7,8,10,19/ :

1. The equations for a corner mesh voltage often tend to produce values which are too low for large grids with many meshes. The error usually is between 10 and 40 percent. In this regard, the simplified formula for factor K_m , Eq. (17) of the Guide, is the worst; it has been known to produce zero or negative values, implying a physically impossible condition in the center of a corner mesh: the electric potential at the earth's surface would have to be equal or greater than that of a current source.

2. The simplified Eq. (22) for K_s produces excessively high step voltages. As a consequence, contradicting design requirements may result from the use of simplified equations, if one attempts to satisfy both the step and touch voltage limit simultaneously. Typically, if the number of grid conductors is increased in order to lower the mesh voltage, the resulting higher K_i - together with a nearly unchanged value of K_s - eventually can offset the effect of an increased conductor length in lowering the average current density per unit of conductor length. Hence, instead of the expected decrease in the step voltage magnitude, an increase results. In all probability, this behavior puzzled many engineers who tried to write a simple computer program based on these equations, and used a logical "if (K_m AND K_s)" type of branch or decision statement in their code in order to exit a calculation loop or finalize the computation when both the required conditions, related to safe values of K_m and K_s , are met.

3. The assumption of an equal current distribution between wires of the grid, combined with the uncertainty about the values of K_i and L , leaves the method open to certain misinterpretations. The most typical is the assumption that only the spacing of corner meshes has to be corrected for K_i calculated by (5), while the number and spacing of inner conductors eventually need not to be changed - if a given design satisfies the safety criteria for some lower value of K_i which is believed to be adequate for inside areas. A failure to account for the effect of a reduced total conductor length and the increase in a linear current density can be disastrous.

4. Neglecting the effect of cross-connections and of ground rods contradicts the facts of life: A grid-rod system is used in most stations, and long ground rods are frequently utilized to reach conductive soil.

5. As the current densities of individual conductors differ more when the number of meshes is increased, a single calculation of the corner mesh voltage alone is nearly irrelevant to a practical design of large grids. Further evaluation of the inner mesh voltages then is necessary for determining a safe grid layout.

Initially, the first two problems were viewed as a matter of unrestrained use, mainly because - implicit in the method - is the assumption that the spacing between conductors is large compared with their diameter and depth of burial. Thus, no method changes were made in the 1976 edition of the Guide.

But three years later, Crawford et al /9/, using a computer, demonstrated that the application of the simplified method failed to produce a sufficiently safe design even in a case which had been the least suspected: the sample calculation for an L-shaped grid design, described in Appendix II of the Guide, pages 39-42. This incident, together with a general progress in computerized modelling of complex grounding systems in multi-layer soils, has set the stage for a major re-assessment of the present method. A further need for the appraisal results from the realization that in installations which include GIS (gas-insulated stations), the simplistic assumptions which are adequate for small conventional stations, often are unrealistic for designing a grounding system which serves compact but electrically large power facility. /26/

2. SCOPE

The purpose of this report - presented in two parts - is to assist and complement the present efforts of Working Group 78.1 of the Distribution Substations Subcommittee in preparing the 1983 edition of IEEE Std 80. In particular, Part I reviews the existing method, rectifies major shortcomings, and ascertains applicability limits of the basic approach. In Part II the method will be extended to evaluate unequally-spaced grounding grids with or without ground rods, allowing either for a uniform soil or a two-layer, high-to-low resistivity medium, with the grid buried in an upper layer, and the rods penetrating a more conductive lower layer. Outline of computing routines, usable in minicomputer and scientific calculator applications, will be also provided.

3. PRINCIPAL CONSIDERATIONS

3.1 Problem Definition

In most substations, the grounding grid is installed in a shallow depth h , usually between 0.5 - 1m, below the earth's surface. For a person walking on the surface, or standing there and touching a grounded metal structure, the safety problem is that of a voltage difference between points P and Q, where his feet are in contact with the earth, and between the potential "Vg" on a grounded metal he might touch; Figure 1.

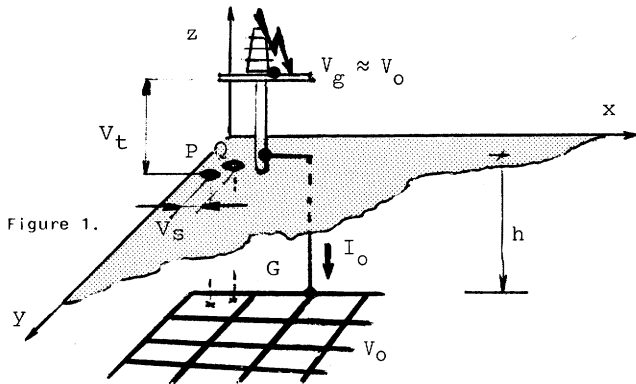


Figure 1. Defining the step and touch voltages "Vs", "Vt", as

$$V_s = \text{Abs}(E_p - E_q) \quad \text{and} \quad V_t = \text{Abs}(E_p - V_0) \quad (6), (7)$$

the problem of a critical surface voltage can be studied in terms of an electric gradient field, produced by a complex electrode G, consisting of a number of rectilinear elements g_1, g_2, \dots, g_n , which are connected to a single current source I_0 . Usually, V_g is put equal to the potential V_0 , carried by the grid.

Behavior of such a system in homogeneous medium of conductivity γ is described by the Laplace formula for a voltage scalar u ,

$$\nabla^2 u = 0 \quad (8)$$

and by several boundary conditions affecting the particular solution of the problem. In more detail, using Cartesian coordinates, when a current density vector J satisfies the linear relationship

$$J(x,y,z) = \gamma E \quad ; \quad \gamma = \text{const.} \quad (9)$$

at any point in a boundless space of (x,y,z) , E then represents a vector field obtained by applying the operator ∇ to the scalar voltage function $u(x,y,z)$ in this space, so that

$$-E = \nabla u(x,y,z) = \left[\frac{\partial u}{\partial x} i + \frac{\partial u}{\partial y} j + \frac{\partial u}{\partial z} k \right] = \text{grad } u \quad (10)$$

By definition, for a constant γ , the field is non-turbulent:

$$\nabla(-E) = \nabla(\nabla u) = \text{rot } E = \begin{bmatrix} i & j & k \\ \partial/\partial x & \partial/\partial y & \partial/\partial z \\ E_x & E_y & E_z \end{bmatrix} = 0 \quad (11)$$

3.2 Major Pitfalls

The method of images is frequently used to overcome the inconvenience of a discontinuity of current flow at the air-earth boundary; but that is just one of many difficulties encountered in the formulation of boundary conditions for a viable solution. Usually, for a complex electrode like the grid G of Figure 1, the condition $u(x,y,z) = \text{const} = V_0$ is required at all points (x_0, y_0, z_0) comprising its surface. However, then the distribution of current densities for all individual elements g_1, g_2, g_3, \dots , becomes formidable problem to calculate, even with the use of a computer. Most of so called exact methods, whether it is a "point-matching" or "matrix method", evolve around the method of moments, described to a great detail in Harrington /14/. The idea is to subdivide each grid element into a number of short segments, presume that the current densities may differ from segment to segment but each are constant along each segment, and solve a set of corresponding equations for $V_j = V$ for all j 's, in order to obtain the currents of k segments, reflecting the step-by-step varying leakage density. Because of symmetries, only a reduced set of n equations with $n < k$ has to be solved; here in a matrix form expressed as

$$[r_{ij} i_k] = V_j \quad ; \quad i, j = 1, 2 \dots, n \quad (12)$$

But, although this problem is of manageable size even for smaller computers /15,16/, two circumstances conspire against successful development of a simplified method for calculating the critical surface potentials above an equally spaced ground grid:

- (1) Singularity phenomenon at geometric extremities.
- (2) Stringency of the linearity criterion for applying a superposition principle on one side, and the inherent incompleteness and often incoherent definition of a simplified mathematical model on the other side.

Solution of problems related to item (1) is particularly difficult in the case of dense grids: According to an established analogy between the resistance of a grid and the capacitance of a rectangular metal plate, the more conductors a grid has, the more its current density distribution resembles that of a plate charge. But, in contrast to the calculation of the total resistance of (or for that matter, capacitance of) the grid by some convenient averaging method - which eventually may disregard end-effect deviations without much of an error - there is no escape from accounting for them in calculating the critical surface voltages near the grid perimeter. To be more specific, consider the potential at point $P(x,y,0)$ above the corner mesh of a grid G, Figure 1. As the grid is near the air-soil boundary, two current density vectors, $J(x_0, y_0, h)$ and $J(x_0, y_0, -h)$, are necessary to quantify the current distribution on the grid and on its image. The potential is

$$V(P) = \frac{1}{4\pi\gamma} \iint_G \frac{[J(x_0, y_0, h) + J(x_0, y_0, -h)] dx_0 dy_0}{\sqrt{(x-x_0)^2 + (y-y_0)^2 + h^2}} w(x,y,x_0,y_0,2h) \quad (13)$$

Above, function "w" symbolizes the role of all mutual resistances between the real and imaginary wire segments and their effect on a current flow toward P. Because the relative magnitude of each current contribution varies inversely with the distance from a sending point, for wires close to P even a small error in values of the calculated current often causes a large cumulative error affecting the result for $V(P)$.

Second problem arises if, for all grid conductors, an equal spacing and uniform leakage current are assumed simultaneously. This double assumption virtually "upgrades" the well-known dilemma of Eq. 12 (requiring all wire segments to be at the same potential, and to leak a current with a constant density along each segment) from the realm of a mere incompatibility to the one of impossibility: implicitly, to violate all basic premises of (11).

And the use of superposition? Although it is true that the voltage-current relation is linear and, in view of (9), the potential on any conductor is a scalar combination of the potentials generated by currents leaking from the individual conductors, these facts do not automatically justify a general applicability of the superposition principle for all manipulations. Consider, for instance, that a current leakage density per unit area varies with the inverse of distance x from the line source of current.

The superposition principle requires that for any functional relationship, the following holds:

$$y(\tau) = \Omega [v(\tau)] \quad ; \quad \text{where } \Omega \text{ is functional operator} \quad (14)$$

$$\Omega [C_1 v_1(\tau) + C_2 v_2(\tau)] = C_1 \Omega [v_1(\tau)] + C_2 \Omega [v_2(\tau)] \quad ; \quad C_1, C_2 = \text{const.} \quad (15)$$

But, for $y(\tau) = \delta(x)$, $v(\tau) = x$, and $\Omega = [J]^{-1}$, the criterion is not met:

$$\frac{1}{C_1 x_1 + C_2 x_2} \neq \frac{1}{C_2 x_2} + \frac{1}{C_1 x_1} \quad (16)$$

Furthermore, as it will be shown later, successive superpositions neglect that a distortion occurs in the electric field due to the presence of other sources. To put it another way: The current ray which emerges in a narrow angle from N-th wire toward the corner mesh on the opposite side of the grid, will never get there - being diverted downward by currents emanating from the other wires.

Figure 2 documents the degradation of a voltage profile which occurs if the basic mathematical model of the present IEEE gradient method is applied to a set of 16 parallel conductors which are in 0.5 m depth below the earth's surface, and spaced 2.45 m apart in a 72 ohm-m soil. The voltage profile is shifted by 1.84 kV to the left side of the voltage scale, to obtain positive values.

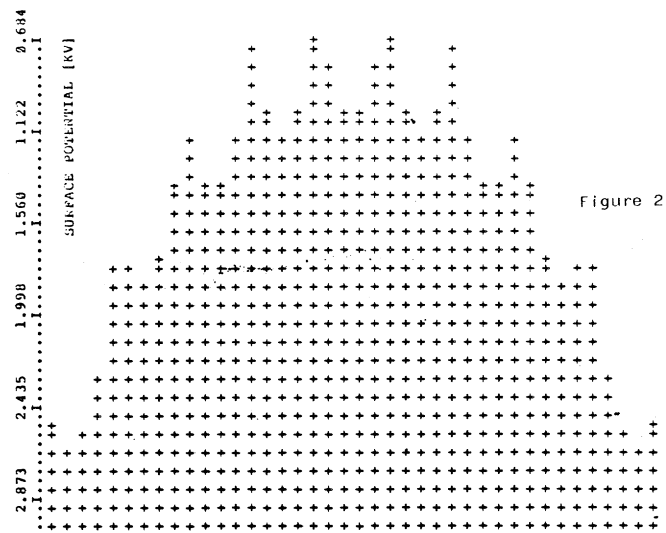


Figure 2.

3.3 What Can Be Accomplished?

Basically, there are three avenues open for the refinement of the IEEE simplified method:

1. Identify error tendencies of the basic model and determine the effect of simplifications; compensate for the errors.
2. Minimize or avoid the singularity problem by design means.
3. Restrict the problem size and assess applicability limits.

As we shall see, all three steps will be taken. For instance, an addition of ground rods along a grid perimeter can accomplish 2., by altering the geometry of the grounding system. As shown in Figure 3, the use of ground rods may be viewed as a conversion of geometry a) into geometry b) in which the corner mesh no longer is in the electrically extreme location of such a combined grid-rod system.

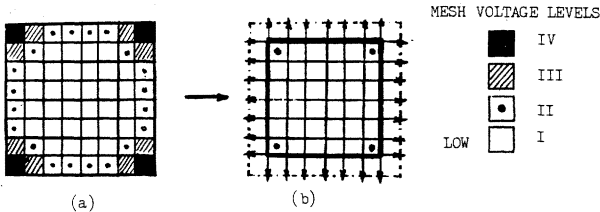


Figure 3.

4. ANALYSIS OF THE PRESENT METHOD

4.1 General Approach

The fundamental Equation (1) for calculating the mesh voltage by the IEEE method, has four basic components. With the exception of one being a constant, the remaining three components are non-trivial multipliers, each being a function of several parameters.

$$E_{mesh} = \prod_{i=1}^4 v(i); \quad \begin{matrix} v(1) = \sigma = \text{const.} \\ v(2) = i = I_0/L \\ v(3) = K_i = 0.172N + 0.65 \\ v(4) = K_m = C \ln(N,D,h,d) \end{matrix} \quad (17)$$

In the particular case of a simplified formula for calculating E_{mesh}, Eq. (16), pp. 19 - 20 of the 1976 edition of the Guide, the analytical formulation of the fourth component is:

$$K_m = \frac{1}{\pi} \ln(D/4\sqrt{hd})(3/4)(5/6) \dots \left(\frac{2N-3}{2N-2}\right) \quad (18)$$

In the forgoing analysis, the components of Equation 17 will be studied at two levels: first, any conceptual deficiency of the basic method will be more or less ignored, and the factor "K_m" will be analyzed with respect to the non-simplified formulation of the model which it is supposed to represent. The approach is to disassemble K_m in its present form, study the pieces, correct any shortcomings of the simplification procedure, and then reassemble K_m and verify the expected effect of the changes made.

Second, the question of deep-rooted deficiencies (which are inherent in the basic model), will be discussed, and certain corrective measures related to the use, and definition of two remaining composite factors "K_i" and "i", will be considered.

Some readers will undoubtedly realize that the entire subject of this analysis can be approached and rigorously treated in terms of such well-founded concepts as of a continuous mapping and of a linear mapping, or better yet, if viewed as a continuous linear transformation, unifying both the topological and algebraic aspects of the former. Nonetheless, in order to reduce the need for a specialized terminology associated with these concepts, a somewhat less precise formulation will be allowed. Given the problem of an electrical gradient field studied - which clearly is that of a vector space and its algebraic structure, the discussion herein will rest just upon two concepts, (coherency and completeness), described in Section 5.

4.2 Choice of Coordinate System

In contrast to the conventional orientation of X-Y-Z coordinates shown in Figure 4a, the coordinate system which will be used in this paper, is that of Figure 4b.

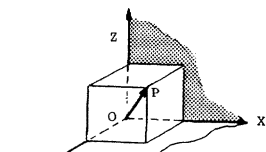


Figure 4a.

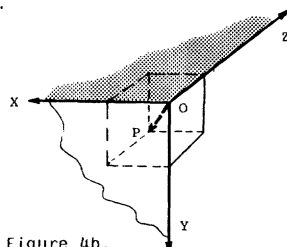


Figure 4b.

As indicated by the alternative positions of a vector P(x,y,z), the rotation of a coordinate "cube" brings the X-Y plane into the plane of this paper. In turn, it also allows to assume that soil fills a half of the infinite space of (x,y,z) for all non-negative y's and to view the X-Z plane as an air-soil boundary. Then, assuming a set of N-parallel conductors to be buried in a depth y = h, and perpendicular to the X-Y plane, such a convention permits to study their gradient fields in the plane of this paper, and the resulting notation becomes fully compatible with that used in the Guide.

4.3 Review of Basic Assumptions

In the Guide, the equations for E_{mesh} were derived with the following assumptions considered valid:

- 1) Conductors extend so far from the X-Y plane that end-effects can be neglected.
- 2) Cross-connections are sufficiently distant to have negligible effect on the current flow and voltage gradients, studied in the X-Y plane.
- 3) Potential drops within the grid are negligible, compared to those within the soil. The absolute potentials of all points on all grid conductors are therefore assumed to be equal.
- 4) Soil is homogeneous and has uniform resistivity.
- 5) Method of images can be used to calculate the effects of "N" conductors buried in depth "h" near the earth-air boundary, (represented by the X-Z plane).
- 6) Each of the "N" real conductors and their images carries the same current; the current dissipation along each conductor is also same. The current "i" flowing into the earth per unit of conductor (real one or image) length, is i = I₀/L.
- 7) Since the soil is homogeneous and the voltage - current relation is linear, the method of superposition can be applied to obtain the magnitudes and directions of current components at any point due to any real or image conductor; each determined separately. All such components can be added vectorially, to give the magnitude and direction of the total current at that point.
- 8) Necessary allowance for a) a somewhat higher unit current in the outer parallel wires - in comparison to the unit current in the wires near the grid center; b) a current increase near the ends of a single wire or in the grid corners (to account for the "end-effect"); c) the presence of cross-connections, special electrodes etc. can be made by means of a corrective factor K_i, the "current irregularity" factor, as described in Section 1.
- 9) D >> h >> d ; D being conductor spacing, h depth of burial, and d conductor diameter.

4.4 Analysis of the Simplified Formula for "E_{mesh}"

The drawback of nice abstractions is the inevitable mismatch between the complexity of reality and the simplicity of assumptions used to describe it. As we will see next, simplifications of the simplifying assumptions help to forget it.

Referring to Appendix 1 of the Guide, and to Appendix 1 and Figure 5 of this paper, it can be stated that the following equation formed the base for all those operations which in the past led to the present simplified formula for E_{mesh}, Eq. (17):

$$E_{mesh} = E_{my} + E_{mx} = \sigma \frac{I_0}{L} K_i [K_{my}(1,1) + K_{mx}(1,N)] \quad (19)$$

where E_{my} is vertical component of the mesh voltage
E_{mx} is horizontal component of the mesh voltage
and

$$K_{my}(1,1) = \frac{1}{2\pi} \ln \left[\frac{4h^2}{4hd - d^2} \right] \quad (20)$$

$$K_{mx}(1,N) = \frac{1}{2\pi} \sum_{k=0}^{N-1} \ln \left[\frac{4h^2 + (2k-1)^2 d^2}{4h^2 + 4(kd)^2} \right] \quad (21)$$

For further convenience, let

$$K_{mx}(1,N) = K_{mx}(1,2) + K_{mx}(3,N) \quad (22)$$

The rationale for using the symbols like K_{my}(1,1) or K_{mx}(1,N) is this: generally, in any factor of (i,j), i is the first and j is the last member of a series; for example, K_{mx}(3,N) represents a composite factor for N-2 conductors, starting with the third and ending with the N-th conductor; Figure 5. Thusly, alluding also to the text of the Guide, there should be no doubt that K_{my}(1,1) represents the effect of a single wire on the voltage difference between the wire and a point on the earth's surface immediately above it. In Figure 5 this wire is the first peripheral conductor in depth "h" on the left side, and the point is X1.

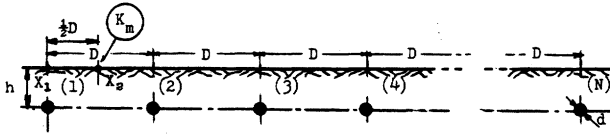


Figure 5.

In order to determine the true relation between the above formula for Emesh and the simplified one, consider now K_m of (18) in the following transcription:

$$K_m = K'_{my}(1,1) + K'_{mx}(1,2) + K'_{mx}(3,N) \quad (23)$$

where $K'_{my}(1,1) = \frac{1}{2\pi} \ln(h/d)$

$$K'_{mx}(1,2) = \frac{1}{2\pi} \ln(D^2/16h^2) = \frac{1}{\pi} \ln(D/4h)$$

$$K'_{mx}(3,N) = \frac{1}{\pi} \ln \left[(3/4)(5/6) \dots \right]$$

Analyzing $K_{my}(1,1)$ and $K'_{my}(1,1)$ first, these expressions become nearly equal for $d/4h$ approaching zero, thus confirming the original constraint of Equation 63 of the Guide, i.e. $4dh \gg d$:

$$K'_{my}(1,1) = \text{Sup. } K_{my}(1,1) \quad 4dh \gg d^2 \quad (24)$$

$$K'_{my}(1,1) = \lim_{d/4h \rightarrow 0} \left[\frac{1}{2\pi} \ln \left[\frac{h}{d(1 - \frac{d}{4h})} \right] \right] = \frac{1}{2\pi} \ln(h/d)$$

$K_{mx}(1,N)$ can be similarly compared with $K'_{mx}(3,N)$ and the latter one identified, barring of one exception, with the effect of $N-2$ wires which are adjacent to the two forming the "corner mesh" in Figure 5, on the voltage difference between points X_1 and X_2 . The exception is, however, a significant one: The Guide implies that $K'_{mx}(3,N)$, the expression which contains series $(3/4)(5/6)(7/8)(9/10) \dots$ etc., results from using the simplifying assumption of $kD + x \gg h$ for $k = 2, \dots, N$. But, the simplifications that had been made, actually put a much more powerful condition $h = 0$ into effect. The limiting operation below, done with the non-simplified series $K_{mx}(i,j)$ of (21), for $i = 3$ and $j = N$, and for h approaching zero, confirms this fact.

$$K'_{mx}(3,N) = \lim_{h \rightarrow 0} \frac{1}{2\pi} \sum_{k=2}^{N-1} \ln \left[\frac{4h^2 + (2k-1)^2 D^2}{4h^2 + 4k^2 D^2} \right] = \frac{1}{\pi} \left(\ln \prod_{k=2}^{N-1} \frac{(2k-1)}{2k} \right) \quad (25)$$

$$= \frac{1}{\pi} \ln \left[(3/4)(5/6)(7/8) \dots (2N-3)/(2N-2) \right]$$

The role of $K'_{mx}(1,2)$ now becomes easier to assess. Declaring formally

$$K_{mx}(1,2) = \frac{1}{4\pi} \sum_{k=0}^1 2 \ln \left[\frac{4h^2 + [(2k-1)D]^2}{4h^2 + 4(kD)^2} \right] = K_{mx}(1) + K_{mx}(2) \quad (26)$$

and using (21) as before, but here for $i = 1$, and $j = 2$, one can observe that a remarkable duality of assumptions is necessary to derive $K'_{mx}(1,2)$ from its non-simplified counterpart. In particular:

- On one hand, to simplify $K_{mx}(1)$, both a non-zero h and $D \gg h$ are required. Only then it is possible to accept

$$K_{mx}(1) = \frac{1}{2\pi} \ln \frac{4h^2 + D^2}{4h^2} = \frac{1}{2\pi} \ln \left[1 + \frac{D^2}{4h^2} \right] \approx \frac{1}{2\pi} \ln \left(\frac{D^2}{4h^2} \right) \quad (27)$$

- On the other hand, for $K_{mx}(2)$ the governing condition is $h=0$. As one may deduct below, unless "D" is approaching infinity, the condition $D \gg h$ is both redundant and less powerful.

$$K'_{mx}(2) = \lim_{h \rightarrow 0} \frac{1}{2\pi} \ln \left[\frac{1}{4} + \frac{3h^2}{4h^2 + 4D^2} \right] = \frac{1}{2\pi} \ln \left(\frac{1}{4} \right) \quad (28)$$

By combining (27) and (28), the desired expression for $K'_{mx}(1,2)$ is obtained:

$$K'_{mx}(1,2) = \frac{1}{2\pi} \ln \left[\left(\frac{1}{4} \right) \left(\frac{D^2}{4h^2} \right) \right] = \frac{1}{2\pi} \ln \left(\frac{D^2}{16h^2} \right) \quad (29)$$

Further combination with (24) produces the familiar first part of formula (18) which, as such, represents the factor K_m for one mesh:

$$K_m = \frac{1}{2\pi} \ln(D^2/16hd) \quad (30)$$

Completion of the above equation by adding the $K'_{mx}(3,N)$ term to obtain (18), is self-evident.

In view of these results one can readily realize that the present simplified formula (18) converts the geometry of Figure 5 into a highly asymmetrical model of Figure 6 below. A full appreciation of this circumstance makes a world of difference in understanding the relatively poor performance of this simplified equation, in a side-by-side comparison with other less simplified or differently simplified versions of the basic mathematical model.

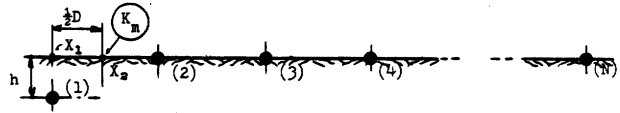


Figure 6.

Tables I and II provide such a comparison made for a series of grid designs, with the computer programmed to proceed with more and more subdivisions of the initial grid pattern, until all results became impractical. The specifics of the series are listed in paragraph 5.5.

4.5 A Better Simplification For K_m

As confirmed by the results of a comparative calculation series, the previous simplification process included a number of questionable decisions. The decision to simplify the $K_{mx}(3,N)$ term of (22) by letting $h=0$, was the most profound one: On one hand, it eliminated both D and h from the series and converted it into a fixed integer sequence, per Equation (25). On the other hand, it made the model highly asymmetrical, and - due to the property of vectorial summations - it also considerably amplified the already excessive tendency of the basic model to show the influence of all conductors which are outside the corner mesh, as being far more pronounced within the corner mesh areas, than what Ohm's law normally permits.

Consequently, two questions concerning (25) can be asked:

First, if the condition $h = 0$ is inadmissible, could a simple corrective term be so devised, as to make the series behave more like that of (21), and get any of possible errors biased against the mentioned undesirable tendencies?

Second, if the first step proves to be feasible, why not try to carry the simplification process to its logical conclusion, and find if any direct analytical solution exists for the product of the numerical sequences so generated?

The answer to both questions is positive. The use of a simple corrective factor $H_m(h, h_0)$ below, has the desired effect on (25).

$$H_m(h, h_0) = 1/\sqrt{1 + h/h_0} \quad ; \quad h_0 = 1 \text{ m} \quad (31)$$

$$H_m(h, h_0) \frac{1}{\pi} \ln \prod_{k=3}^N \frac{(2k-3)}{(2k-2)} \approx \frac{1}{2\pi} \sum_{k=2}^{N-1} \ln \left[\frac{(2k-1)^2 D^2 + 4h^2}{4k^2 D^2 + 4h^2} \right] \quad (32)$$

And indeed, as derived in Appendix III, there exists a very good estimate for the product of a finite series $(3/4)(5/6)(7/8) \dots$, which becomes exact for infinite N ; Eq. (III-17).

Therefore, a much briefer expression now can be used to approximate $K_{mx}(3,N)$:

$$H_m(h, h_0) \cdot K'_{mx}(3,N) = \frac{1}{2\pi} \frac{1}{\sqrt{1 + h/h_0}} \ln \left[\frac{8}{\pi(2N-1)} \right] \quad (33)$$

It is rather interesting to see what happens if (31) is combined with the old improperly reduced term (25) to obtain an "h-adjusted" asymmetrical formula for Emesh, stated below:

$$E_{\text{mesh}} = \frac{\sigma T \Omega}{\pi L} \left[\ln \left(\frac{D}{4\sqrt{hd}} \right) + \frac{1}{\sqrt{1+h/h_0}} \ln \left(\frac{3}{4} \right) \left(\frac{5}{6} \right) \dots \right] K_1 \quad (34)$$

Columns EM1 and EM1* in Tables I-II, document the performance of the above series with respect to the old one. Reading column EM1* for the results of (34), one can see that eventually a better performing simplified formula could have been developed in the past.

However, as shown in Appendix II, an equally simple formula can be derived for a symmetrical model of the corner mesh per Fig. 7.



Figure 7.

This new formula for Km which combines (11-10) of Appendix 11 and (33) above, is:

$$K_m = \frac{1}{2\pi} \left[\ln \left(\frac{D^2}{16hd} + \frac{(D+2h)^2}{8Dd} - \frac{h}{4d} \right) + \sqrt{\frac{1}{1+h/h_0}} \ln \left(\frac{8}{\pi(2N-1)} \right) \right] \quad (35)$$

Its performance is shown in column EMNEW1, Tables I and II.

5. IMPROVED EQUATIONS

5.1 Fundamental Modeling Concepts

Viewing the relationship between a selected grounding system and some corresponding mathematical model as one transformation, involving the "original" system defined by one set of parameters and a "transformed" one, defined by another parameter set - that of the model, the following concepts hold true:

Lemma (i) - A model is complete if and only if a direct correspondence exists between the parameters of the original set O(p) and those of the model set T(p'), and this correspondence is one-to-one.

Lemma (ii) - Let the respective results of calculations based on O(p), and those based on T(p'), be functions R(O) and R'(T), as follows: both are defined in the domain of Cartesian coordinates {x,y,z}. Then the model is coherent if for an error function $\lambda(x,y,z) = Abs [R(O) - R'(T)]$, it holds: $\lambda(\partial^2/\partial x^2, \partial^2/\partial x\partial y, \dots, \text{etc.}) = C$, for any test $\lambda(\alpha,\beta,\gamma)$ such that $\alpha, \beta, \gamma \in \{x,y,z\}$.

Obviously, the coherency requires that an error function is well behaving, i. e. monotonously increasing, decreasing or constant. With reference to figure 2, it is submitted without proof that the fundamental mathematical model of the IEEE gradient method is both incomplete and incoherent.

5.2 Flaws and Correctability of the Basic Model

As it can be determined from the comparison of columns EM-3 and EM-4, Tables I-11, a full representation of the basic model, per Appendix 1, eq's. (1-7) and (1-18), as used in column EM-4, does not perform as good as equation (19), shown in column EM-3. And, both eventually become negative for high N's. Why is this so?

There are four principal reasons: first, the difference results from neglecting N-2 conductors in the Ey term of (19). In spite of the fact that in assessing the Ey contribution of wires which are remote from the corner mesh, most of the wires and their images appear as about equidistant from the point above the corner mesh, their effect still is significant enough to further amplify the already too strong effect of N conductors in the Ex term. As a consequence, equation (1-18) is more erroneous than (19). However, the best model is that with not one but two first wires taken into account in the Ey term, eq. (36). This is verifiable with the use of a Fortran subroutine FULSER below, by setting NY equal to 1, 2, 3, ..., etc., and to N, respectively.

```

SUBROUTINE FULSER(CKM,EXF,EYF,CDIA,DPTH,SPAC,NX,NY,PI)
-----
TERM(A,B,C,D)=(A*A+B*B)/(C*C+D*D)
T1=1.
T2=1.
T3=1.
RA=CDIA/2.
RB=2.*DPTH-RA
DO 1 M=1,NX
DK=SPAC*FLOAT(M-1)
DM=SPAC*FLOAT(2*M-3)/2.
T1=11*TERM(DPTH,DM,DPTH,DK)
IF(M.GT.NY)GO TO 1
T2=12*TERM(DPTH,DK,RA,DK)
T3=13*TERM(DPTH,DK,RA,DK)
1 CONTINUE
EXF=ALOG(T1)/(2.*PI)
EYF=(ALOG(T2)+ALOG(T3))/(4.*PI)
CKM=EXF+EYF
RETURN
END
-----
* A FUNDAMENTAL MODEL OF THE GUIDE 80 GRADIENT METHOD (36)
* NX IS NUMBER OF WIRES TAKEN INTO ACCOUNT FOR EX COM- (37)
* PONENT, NY IS THAT FOR EY COMPONENT.
    
```

Here, the notation is:
 CKM Km
 EXF Km*(1,NX)
 EYF Km*(1,NY)
 CDIA d

Figure 8.

Second, the use consecutive superpositions neglects the influence of other wires present. In order to restore the validity of (11), a number of additional fictitious sources would have to be introduced to compensate for this conceptual deficiency.

Third, contrary to assumptions 2 and 8, since the length of cross-connections is included in the total wire length L, these cross-connections are not neglected but converted into extra extensions of the remaining N conductors. Because $i = I_0/L$, this results in doubling of the area size and a reduction of the conductor length per unit of area. Also, this method provides no compensation for an increase in the mutual resistance between densely spaced wires which would cause a reduction in the calculated current flow from the inner conductors toward the corner mesh. The net outcome is a disproportionately high current saturation of the soil between the two parallel wires forming the "corner mesh", which far exceeds the possible range of current densities per unit of area occurring there during a fault. This applies to all versions of the model.

The name of Schwarz must be mentioned here: his clear perception of the significance of a conductor density per unit of a grid covered area, as well as his approach to the development of a simplified method for determining the resistance of grid-rod systems are as much of interest today, as twenty-five years ago. /22/

Fourth, the application of the Ki factor upsets Ohm's law but not much is wrong with the factor formula itself. In fact, contrary to what many believed, the straight-line function of Ki is consistent with the model used. However, the problem is as follows:

$$\frac{I_0}{R_g} = \frac{iL}{R_g} \neq K_i \frac{iL}{R_g} \text{ if } K_i > 1 \quad (38)$$

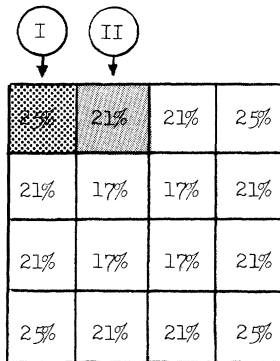
Obviously the only way to satisfy the left side of (37) above, is to use a second corrective factor for the average current of conductors outside the corner mesh, which has to be less than one:

$$\frac{iL}{R_g} = \frac{K_{i1} L_1 + K_{i2} L_2}{R_g} i; \text{ for } L_1 + L_2 = L \text{ and } K_{i1} < 1 \quad (39)$$

5.3 Role of Ground Rods

So far no attention has been paid to the fact that, in practice, a typical grounding system includes not only the horizontal conductors forming a grid, but also a substantial number of ground rods connected to it. The foremost reason for this omission is, of course, that the principal model has no provisions for recognizing the individual grounding rods as such. In fact, since a set of N parallel conductors of undetermined individual lengths is substituted for the grid and rods, seemingly a very little can be done in accounting for the presence of ground rods -- and even less so in regarding the effect of their allocation within the grid. But, no matter how discouraging this appears to be, first consider the following three basic cases of an identical grid: 1) with no rods, 2) with 24 rods along perimeter, and 3) with 24 rods spread evenly within the grid area; figures 9, 9a, 9b, respectively.

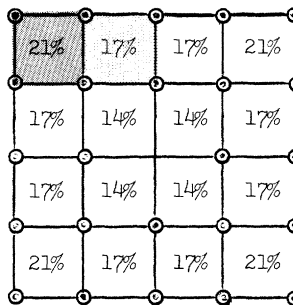
The pertinent data are: soil resistivity 100 ohm-m, 40 m X 40 m grid area, total length of grid conductors 400 m, 24 ground rods each long 4.1 m, depth of grid burial 0.5 m, and the diameter of both horizontal and vertical electrodes 0.02 m.



GRID #1

$I_0 = 1,000 \text{ A}$
 $R_g = 1.210 \Omega$
 $E_{mI} = 303.8 \text{ V}$
 $E_{mII} = 251.4 \text{ V}$
 $GPR = 1,210 \text{ V}$

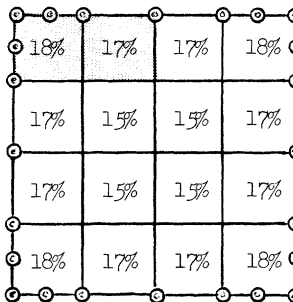
Figure 9.



GRID #2

$I_0 = 1,000 \text{ A}$
 $R_g = 1.119 \Omega$
 $E_{mI} = 234.2 \text{ V}$
 $E_{mII} = 192.9 \text{ V}$
 $GPR = 1,119 \text{ V}$

Figure 9a.



GRID #3

$I_0 = 1,000 \text{ A}$
 $R_g = 1.100 \Omega$
 $E_{mI} = 201.5 \text{ V}$
 $E_{mII} = 191.7 \text{ V}$
 $GPR = 1,100 \text{ V}$

Figure 9b.

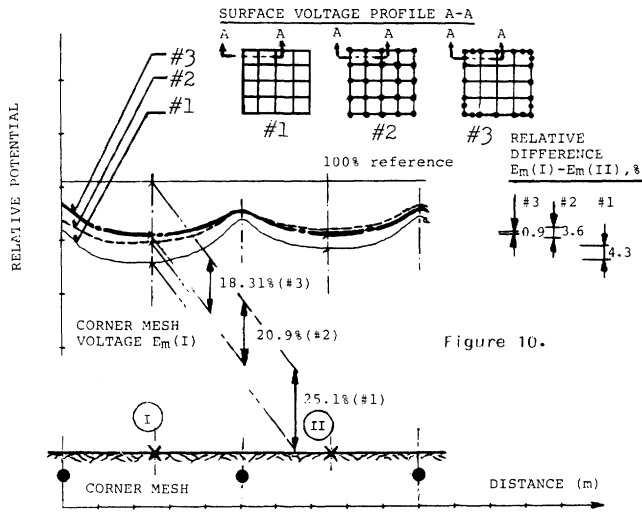


Figure 10.

As it can be deduced from the results of a computer simulation, shown in Figure 10,

- if the rods are placed exclusively along the perimeter, there is a very small difference between the surface potentials of the corner mesh and of the other meshes;
- if the rods are spread evenly over the entire grounding area, or worse, if no rods are used at all, the difference is substantial. In the former case, the overall potential rise is lower because of the increase in the total buried length;
- the "crowding" of ground rods in the grid corners, has no adverse effect on the grid resistance. In fact, the resistance of GRID #3 is a little lower than that of GRID #2. Needless to say, this result still may be somewhat of a shock to many.

5.4 New Simplified Formuli for "Emesh"

It is well known that if the number of grid meshes is increased, a current density in the peripheral conductors exponentially increases, attaining an extremely high value in the grid corners. But, equally important is the fact that while the current density values in the interior region of the grid change very little, the relative size of this electrically "flat" inner area is increased. And, precisely the latter phenomenon is also the root of a somewhat paradoxical conclusion, concerning the applicability of simplified equations: Although the basic IEEE model was originally developed in disregard of any role of ground rods but their buried length, a grid - rod combination with ground rods placed predominantly along the perimeter is the only design concept for which this simplified method is analytically most suitable.

Hence, reflecting the experience with the use of ground rods described previously, the following equations can be established:

$$E_{mesh} = \sigma I_o K_i \left[\frac{1}{2\pi L} K_{mxy}(1,2) + \frac{1}{\pi L} K_{ii} H_m(h, h_o) K_{mx}^*(3,N) \right] \quad (40)$$

where, in addition to the already explained symbols,

K_{ii} is correction factor for inner area currents

L_c is total length of horizontal grid conductors

L_r is total length of ground rods

$L = L_c + 1.15 L_r$ for grids with rods along perimeter and $K_{ii} = 1$;

$L = L_c + L_r$ for grids with rods evenly spread over A, and $K_{ii} = (2N)^{-2/N}$

The 1.15 multiplier in (39) reflects the theoretical premise of a relatively higher efficiency of ground rods in emitting current into the earth - in comparison to an equivalent length of grid conductors; /20,21,24/.

In a more explicit form, for a grid with rods along perimeter, the equation is (41):

$$E_{mesh} = \frac{\sigma}{2\pi(L_c + 1.15L_r)} K_i I_o \left[\ln \left(\frac{D^2}{16hd} + \frac{(D+2h)^2}{8Dd} - \frac{h}{4d} \right) + \frac{1}{\sqrt{1+h/h_o}} \ln \frac{8}{\pi(2N-1)} \right]$$

Alternatively, for a grid without ground rods, or with the rods evenly spread within the entire grid area, the equation becomes (42):

$$E_{mesh} = \frac{\sigma K_i I_o}{(L_c + L_r) 2\pi} \left[\ln \left(\frac{D^2}{16hd} + \frac{(D+2h)^2}{8Dd} - \frac{h}{4d} \right) + \frac{1}{(2N)^{2/N} \sqrt{1+h/h_o}} \ln \frac{8}{\pi(2N-1)} \right]$$

As it can be seen in columns EMNEW1 and EMNEW2 in Tables I-II, the effect of a semi-empirical factor K_{ii} is not too drastic, yet producing adequate compensation for an excessive magnitude of the average current of N-2 conductors near the corner mesh.

5.4 Grounding Resistance Formula

In the Guide, the calculation of a grounding resistance is divorced from the mathematical model used in the gradient analysis, and the following simple formula is provided:

$$R_g = \sigma \left(\frac{1}{4x} + \frac{1}{L} \right) \quad \text{for } h = 0 ; \quad x = \sqrt{A/\pi} \quad (43)$$

Although the depth of burial is not mentioned, it is reasonable to assume $h = 0$; for an infinite L, the formula becomes that of a metallic plate at zero depth. In order to obtain a correction for non-zero but shallow depths in the usual .25 - 2.5 m range, the above expression can be combined with another semi-empirical formula for a plate, suggested by Laurent in reference /2/ :

$$R_p = \sigma \frac{1}{8x} \left(1 + \frac{x}{2.5h+x} \right) \quad \text{for non-zero } h \quad (44)$$

Besides having h as a parameter, the resulting formula has one more advantage: it is relatively easy to remember.

$$R_g(h) = \sigma \left[\frac{1}{L} + \frac{1}{\sqrt{20A}} \left(1 + \frac{1}{1+h/20A} \right) \right] \quad (45)$$

The above formula compares equally well with a more complex equations of Schwarz (not shown) and of Nahman; see column RGENW and column RGAH in Tables I-II, respectively.

5.5 Comparative Computer Series - Tables I and II

A series of computer runs has been used to compare the performance of the IEEE model and of the equations proposed by other authors, and to ascertain the effect of various simplifications on the basic formula for Emesh. Although these calculations were made for depths ranging from 0.25 m to 2.75 m, in 0.25 m steps, only the results for 0.25 m and 2.5 m have been tabulated. Specific parameters and design data pertaining to Tables I-II, are:

COLUMN	EQUATION	DESCRIPTION
EM-1	(17-18)	old simplified formula of Guide 80, Eq. 16
EM-1*	(34)	same as EM-1, but h-adjusted by H_m , per (31)
EM-1T	-	same as EM-1, but using Thapar's K_i per (46)
EM-1N	-	same as EM-1, but using Nahman's K_i per (52)
EMZUK	(51)	Zukerman's formula based on Guide 80, Eq. 16
EM-2	(19-21,25)	partly simpl. formula of Guide 80, Appdx. I
EM-2*	-	same as EM-2, but h-adjusted by H_m , per (31)
EM-3	(19)	non-simplified formula of Guide 80, Appdx. I
EM-4	(1-18)	fundamental model having N of $E_x + E_y$ terms
EMZIN	(56)	Zink's eq. for $K_i K_m$ product by correlation
EMNAH	(54)#	Nahman Equation based on $K_i K_m$ formula (54)
EMNEW1	(41)	new symmetrical formula - rods along perimr.
EMNEW2	(42)	new symmetrical formula - rods evenly spread
RGNEW	(45)	new simplified formula for grid resistance
RGAH	(53)	Nahman's grid resistance formula

#) Note: Since Eq. (54) is based on $h=0.5$ m, EMNAH values have been approximated as follows:

$$Eq.(54) \times RGAH (h = 0.25m, \text{ or } 2.5m) / RGAH (h = 0.5m)$$

The printed values EM-1 to EMNEW2 are in volts, RGNEW and RGAH are in ohms; D is spacing in meters, N number of || conductors. Design Data: Grid area 40 m x 40 m, soil resistivity 100 ohm-m, conductor diameter 0.01m (10 mm); grid current is 1 kA.

6. REVIEW OF RELATED WORK BY OTHERS

6.1 Thapar and Nagar's Formula for K_i , Reference /18/

In order to establish the validity of the IEEE method for larger grids, in 1976 Thapar & Nagar performed tests on model grids in an electrolytic tank, extending the previous Koch's experiments with simple square grids (64 meshes maximum), to 256 meshes. Referring partly to the outcome of these tests, and partly to the results of an analytical solution of the current distribution in a set of N parallel wires, they recommend to use an altered K_i curve for higher N's.

$$K_i = 0.22N + 0.3 ; \quad \text{for } 5 \leq N \leq 21 \quad (46)$$

in conjunction with the simplified formula for K_m , Equation (18). Since the analytical method is based on a simultaneous calculation of N different currents, this part of the reference will be discussed in more detail in Part II. However, the effect of (46) on the simplified formula for Emesh is shown in column EM11, in Tables I-II. Compared to column EM1, the values of fmesh are approximately 10% higher, if (46) is used in (17).

6.2 Zukerman's Equation, Reference /8/

In 1978, attempting to rationalize the procedures of the Guide, Zukerman developed a semi-graphical method for the design analysis of grounding grids. In order to make the simplified formula for Emesh suitable for graphical applications, he used the following expressions for K_i and K_m :

DEPTH = 0.25 (M)

TABLE I

GRID SUBDIVISION SERIES

N	D	EM-1	EM-1*	EM-1T	EM-1N	EMZUK	EM-2	EM-2*	EM-3	EM-4	EMZIN	EMNAH	EMNEW1	EMNEW2	RGNEW	RGNAH
3	20.0	667.7	672.4	667.7	615.2	664.3	667.7	672.4	668.5	668.5	717.2	536.4	667.5	700.0	1.519	1.518
4	13.3	496.4	503.0	496.4	471.1	491.4	496.5	503.1	497.2	497.2	536.4	400.9	501.3	540.2	1.415	1.404
5	10.0	397.6	405.2	397.6	392.6	392.5	397.7	405.3	398.4	398.4	433.4	345.9	405.3	446.1	1.353	1.343
6	8.0	332.4	340.7	320.1	344.9	327.7	332.6	340.9	333.3	333.3	366.4	309.2	342.1	383.2	1.311	1.306
7	6.7	285.7	294.5	283.5	314.1	281.4	285.9	294.7	286.7	286.6	318.8	283.1	296.8	337.5	1.281	1.283
8	5.7	250.1	259.4	254.3	293.6	246.4	250.4	259.7	251.3	251.2	282.9	263.5	262.5	302.5	1.259	1.266
9	5.0	222.0	231.6	230.3	279.7	218.7	222.3	231.9	223.3	223.2	254.8	248.3	235.4	274.5	1.242	1.255
10	4.4	198.9	208.8	209.8	270.2	196.1	199.4	209.2	200.5	200.2	231.9	236.1	213.3	251.5	1.228	1.206
11	4.0	179.5	189.7	192.1	263.8	177.2	180.1	190.2	181.3	181.0	212.9	226.2	194.8	232.1	1.216	1.240
12	3.6	163.0	173.3	176.5	259.6	161.0	163.6	174.0	164.9	164.6	196.8	217.9	179.1	215.5	1.207	1.235
13	3.3	148.5	159.1	162.6	256.7	147.0	149.3	159.8	150.7	150.4	182.8	210.8	165.4	201.0	1.199	1.231
14	3.1	135.8	146.5	150.1	324.8	134.6	136.6	147.4	138.3	137.8	170.6	204.8	153.5	188.2	1.192	1.228
15	2.9	124.4	135.3	138.6	403.8	123.6	125.4	136.3	127.2	126.7	159.8	199.6	142.8	176.8	1.186	1.226
16	2.7	114.1	125.2	128.1	472.5	113.7	115.2	126.3	117.2	116.6	150.1	195.1	133.3	166.6	1.181	1.224
17	2.5	104.8	116.0	118.4	532.0	104.7	106.1	117.3	108.2	107.5	141.4	191.1	124.7	157.3	1.176	1.223
18	2.4	96.2	107.6	109.4	582.9	96.5	97.7	109.0	100.0	99.3	133.4	187.5	116.9	148.8	1.172	1.222
19	2.2	88.3	99.9	101.0	625.9	88.9	89.9	101.5	92.4	91.7	126.2	184.3	109.7	141.0	1.169	1.221
20	2.1	81.0	92.7	93.1	661.1	81.9	82.8	94.5	85.5	84.6	119.5	181.4	103.1	133.8	1.165	1.220
21	2.0	74.2	86.0	85.7	688.9	75.4	76.2	88.0	79.1	78.2	113.3	178.8	97.0	127.1	1.162	1.220
22	1.9	67.9	79.8	78.7	709.3	69.3	70.0	82.0	73.1	72.1	107.6	176.4	91.4	120.9	1.160	1.219
23	1.8	61.9	73.9	72.0	722.4	63.5	64.3	76.3	67.6	66.5	102.2	174.3	86.1	115.1	1.157	1.219
24	1.7	56.3	68.4	65.7	728.2	58.2	58.9	71.0	62.4	61.2	97.2	172.3	81.2	109.7	1.155	1.219
25	1.7	51.0	63.2	59.7	726.7	53.1	53.8	66.0	57.5	56.2	92.5	170.5	76.6	104.6	1.153	1.219
26	1.6	45.9	58.3	54.0	717.8	48.3	49.0	61.3	52.9	51.5	88.0	168.8	72.2	99.8	1.151	1.219
27	1.5	41.1	53.6	48.5	701.5	43.7	44.4	56.9	48.6	47.1	83.8	167.2	68.2	95.2	1.149	1.219
28	1.5	36.6	49.1	43.2	677.6	39.4	40.1	52.7	44.6	43.0	79.8	165.8	64.3	91.0	1.147	1.219
29	1.4	32.2	44.9	38.2	646.0	35.2	36.0	48.7	40.7	39.0	76.1	164.4	60.6	86.9	1.146	1.219
30	1.4	28.0	40.8	33.3	606.8	31.2	32.1	44.9	37.1	35.2	72.5	163.2	57.2	83.0	1.144	1.219
31	1.3	24.0	36.9	28.6	559.6	27.4	28.4	41.3	33.6	31.7	69.0	162.0	53.9	79.4	1.143	1.219
32	1.3	20.2	33.1	24.1	504.4	23.8	24.9	37.8	30.3	28.2	65.7	160.9	50.7	75.9	1.142	1.219
33	1.3	16.5	29.5	19.7	441.1	20.3	21.5	34.5	27.2	25.0	62.6	159.8	47.8	72.5	1.141	1.219
34	1.2	13.0	26.1	15.5	369.6	16.9	18.3	31.4	24.2	21.9	59.6	158.9	44.9	69.4	1.140	1.219
35	1.2	9.5	22.7	11.4	289.6	13.7	15.2	28.4	21.3	18.9	56.7	157.9	42.2	66.3	1.139	1.220
36	1.1	6.2	19.5	7.5	201.2	10.5	12.2	25.5	18.6	16.1	53.9	157.1	39.6	63.4	1.138	1.220
37	1.1	3.0	16.4	3.7	104.1	7.5	9.4	22.7	16.0	13.4	51.2	156.2	37.1	60.6	1.137	1.220
38	1.1	-0.0	13.4	-0.1	-1.8	4.6	6.7	20.1	13.5	10.7	48.7	155.5	34.7	57.9	1.136	1.221
39	1.1	-3.0	10.4	-3.7	-116.6	1.7	4.1	17.5	11.1	8.2	46.2	154.7	32.4	55.4	1.135	1.221
40	1.0	-6.0	7.6	-7.2	-240.4	-1.0	1.5	15.1	8.9	5.8	43.8	154.0	30.2	52.9	1.134	1.221
41	1.0	-8.8	4.9	-10.6	-373.3	-3.7	-0.9	12.8	6.7	3.5	41.4	153.4	28.1	50.5	1.133	1.221
42	1.0	-11.5	2.2	-13.9	-515.6	-6.3	-3.2	10.5	4.6	1.3	39.2	152.7	26.1	48.2	1.133	1.222
43	1.0	-14.2	-0.4	-17.2	-667.2	-8.8	-5.4	8.3	2.6	-0.9	37.0	152.1	24.2	46.0	1.132	1.222
44	0.9	-16.8	-2.9	-20.4	-828.4	-11.2	-7.6	6.2	0.6	-3.0	34.9	151.5	22.3	43.9	1.131	1.222
45	0.9	-19.3	-5.4	-23.5	-999.2	-13.6	-9.7	4.2	-1.2	-5.0	32.8	151.0	20.5	41.8	1.131	1.222
46	0.9	-21.7	-7.8	-26.5	-1179.7	-16.0	-11.7	2.3	-3.0	-6.9	30.8	150.4	18.7	39.9	1.130	1.223
47	0.9	-24.1	-10.1	-29.4	-1370.2	-18.2	-13.6	0.4	-4.7	-8.7	28.9	149.9	17.1	38.0	1.129	1.223
48	0.9	-26.5	-12.4	-32.3	-1570.6	-20.4	-15.5	-1.4	-6.4	-10.5	27.0	149.4	15.4	36.1	1.129	1.223
49	0.8	-28.8	-14.6	-35.1	-1781.1	-22.6	-17.3	-3.1	-8.0	-12.3	25.2	149.0	13.9	34.3	1.128	1.224
50	0.8	-31.0	-16.8	-37.9	-2001.9	-24.7	-19.0	-4.8	-9.5	-14.0	23.4	148.5	12.3	32.6	1.128	1.224

SOLID PLATE APPROX.

0	0.0	-284.2	-283.5	-363.4	*****	-253.5	-203.7	-203.0	-189.5	-300.0	-160.2	127.6	-190.7	-189.9	1.118	1.313
---	-----	--------	--------	--------	-------	--------	--------	--------	--------	--------	--------	-------	--------	--------	-------	-------

DEPTH = 2.50 (M)

TABLE II

GRID SUBDIVISION SERIES

N	D	EM-1	EM-1*	EM-1T	EM-1N	EMZUK	EM-2	EM-2*	EM-3	EM-4	EMZIN	EMNAH	EMNEW1	EMNEW2	RGNEW	RGNAH
3	20.0	489.6	510.3	489.6	460.8	486.2	493.4	514.1	498.1	496.7	647.3	450.3	528.2	547.6	1.413	1.274
4	13.3	343.2	372.3	343.2	339.6	338.7	350.8	379.9	359.0	356.1	471.2	341.9	399.7	423.0	1.308	1.197
5	10.0	259.2	293.0	259.2	274.2	255.1	271.9	305.7	283.4	278.8	371.1	298.2	329.0	353.4	1.246	1.158
6	8.0	204.0	240.8	196.5	233.9	200.4	223.0	259.8	237.1	230.7	306.0	268.8	284.9	309.5	1.204	1.136
7	6.7	164.3	203.4	163.1	206.5	161.4	190.6	229.7	206.5	198.3	259.7	247.7	255.3	279.6	1.174	1.122
8	5.7	134.1	174.9	136.4	186.2	131.8	168.4	209.2	185.2	175.3	224.9	231.8	234.4	258.2	1.152	1.114
9	5.0	110.1	152.4	114.2	169.7	108.4	152.6	194.9	169.9	158.3	197.6	219.4	219.0	242.3	1.135	1.109
10	4.4	90.3	133.9	95.3	155.1	89.2	141.2	184.7	158.5	145.3	175.4	209.5	207.3	230.1	1.121	1.106
11	4.0	73.7	118.3	78.9	146.4	73.1	132.6	177.2	149.7	135.1	156.9	201.3	198.3	220.6	1.110	1.104
12	3.6	59.4	105.0	64.3	187.6	59.2	125.9	171.6	142.9	126.9	141.2	194.6	191.2	212.9	1.100	1.103
13	3.3	46.8	93.4	51.3	206.3	47.2	120.6	167.2	137.5	120.2	127.6	188.8	185.4	206.7	1.092	1.102
14	3.1	35.7	83.1	39.5	204.6	36.5	116.3	163.7	133.1	114.6	115.7	183.9	180.7	201.5	1.085	1.102
15	2.9	25.7	73.9	28.7	183.5	26.9	112.7	160.8	129.4	109.9	105.1	179.6	176.9	197.2	1.079	1.103
16	2.7	16.7	65.6	18.8	144.0	18.3	109.6	158.4	126.4	105.9	95.7	175.8	173.7	193.5	1.074	1.103
17	2.5	8.5	58.0	9.6	86.2	10.4	106.8	156.4	123.8	102.4	87.2	172.5	171.0	190.4	1.069	1.104
18	2.4	0.9	51.1	1.0	10.4	3.2	104.3	154.6	121.6	99.3	79.4	169.6	168.7	187.7	1.065	1.105
19	2.2	-6.1	44.7	-7.0	-83.3	-3.5	102.1	152.9	119.6	96.6	72.3	167.0	166.7	185.4	1.062	1.106
20	2.1	-12.6	38.8	-14.5	-195.2	-9.7	100.0	151.5	117.9	94.2	65.8	164.6	165.0	183.3	1.058	1.107
21	2.0	-18.7	33.3	-21.6	-325.4	-15.5	98.1	150.1	116.5	92.0	59.7	162.5	163.6	181.5	1.055	1.108
22	1.9	-24.5	28.1	-28.3	-474.0	-21.0	96.3	148.9	115.2	90.1	54.1	160.5	162.3	179.9	1.053	1.109
23	1.8	-29.8	23.2	-34.7	-641.4	-26.1	94.6	147.7	114.0	88.3	48.9	158.7	161.2	178.5	1.050	1.110
24	1.7	-34.9	18.6	-40.8	-827.8	-30.9	93.0	146.6	112.9	86.7	44.0	157.1	160.2	177.2	1.048	1.111
25	1.7	-39.7	14.3	-46.6												

$$K_i \approx (m+5)/6 \tag{47}$$

$$K_m = \frac{1}{\pi} [\ln(S/4\sqrt{hd}) - 1.45 \ln(m)] \tag{48}$$

where, in addition to the symbols already defined before,

m is the number of meshes along a grid side. For a square grid, or for a rectangular grid with "N" parallel conductors both in the east-west and the north-south directions, m = N - 1.

S is the length of a square grid, or the short side of a rectangular grid.

Of interest is the expression for Km, since it contains a non-trivial simplification of the series (3/4)(5/6)(7/8) ... , of the original IEEE formula, Eq. (17).

A substitution of (N-1)D for "S" and N-1 for "m" in (48), yields

$$K_m = \frac{1}{2\pi} [\ln(D^2/16hd) + 2(1-1.45) \ln(N-1)] \tag{49}$$

which can be further rearranged into

$$K_m = \frac{1}{2\pi} \ln(D^2/16hd) - \frac{0.45}{\pi} \ln(N-1) \tag{50}$$

From the last expression, it can be seen that Zukerman's conversion retains exactly the combination of K'my(1,1) and K'mx(1,2) terms of Eq. (30), but substitutes a simple numerical approximation for the K'mx(3,N) term:

$$K_{mx}^*(3,N) \approx -(0.45/\pi) \ln(N-1) \tag{51}$$

This approximation is reasonably accurate for most practical calculations, though lacking the qualities of supremacy and convergence of the similar expression (33) developed in this paper. Figure 11.

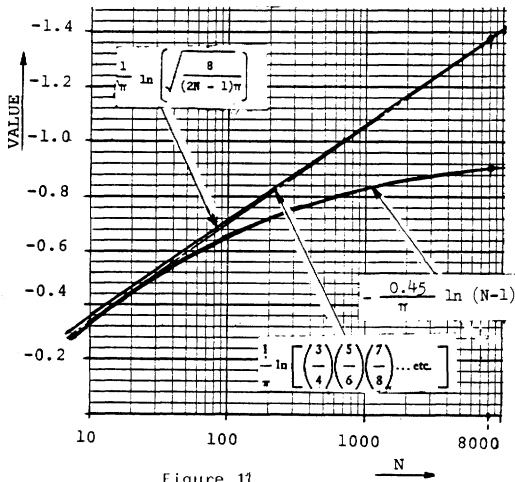


Figure 11.

In the whole, however, the Zukerman's formulation suffers from and has the same deficiencies as the original IEEE formula. In Tables 1-11, column EMZUK provides ample evidence for this conclusion. (Of course, the same comment applies to columns EM1T and EM1N as well.)

6.3 Simplified Equations of Nahman and Skuletich

Asserting that the IEEE simplified formula for E_{mesh} provides satisfactory results for conductor spacings exceeding 5 m, but yields results which are too low for denser spacings and burial depths greater than 0.5 m, in reference /10/ Nahman et al. suggested to replace the factor Ki in (18) by a more progressive function, stated below.

$$K_i = 0.155 N + 0.58 + \lambda_i \tag{52}$$

where

$$\lambda_i = \begin{cases} 0.680 \theta - 8.55 & \text{for } \theta > 16.3 \\ 0.155 \theta & \text{for } \theta \leq 16.3 \end{cases}; \theta = (N)^3(\sqrt{A})^{-1.25}(h)10/\sqrt{A}$$

Furthermore, in a related paper /11/, they presented the following formula for the product of Ki and Km in Equation (1), and for calculating the resistance of rectangular grids:

$$R_g = \sigma \left[\frac{0.53}{\sqrt{A}} + \frac{1.75}{L^3 N} \right] \left[1 - 0.8 \left(\frac{100hd}{N\sqrt{A}} \right)^{\frac{1}{4}} \right] \tag{53}$$

$$K_i K_m = 0.0248(\sqrt{A} - 10)^{0.72} + \frac{1}{10} (\sqrt{A}/D - 2.5) + 0.9 \tag{54}$$

The performance of (52),(54),(53) is shown in Tables 1-11, in columns EM1N, EMNAH, RGMAL, respectively. As it can be observed, while (54) is well-behaved function which remains positive throughout the entire test series, the use of (52) in conjunction with Km of (18) proves to be troublesome; with increasing N and decreasing D, the values of E_{mesh} go down, up, and down again, before becoming negative.

6.4 Note on Work by Voronina, Reference /21/

Although Armstrong and Simpkin included in their experiments the case of ground rods placed along a grid perimeter /24/, it was Voronina who fully recognized the significance of this grid-rods configuration in controlling the surface voltage above the grid. In 1969, she conducted tests with model grids for 1 - 32 meshes, including grids with and without cross-connections, with or without ground rods, and developed several analytical expressions in correlation to the experimental results, which allow to find the ground resistance and the step and touch potentials of a grounding system as a product of several tabulated coefficients.

6.5 Zink's Km Ki Product

Similarly as Voronina, but with one difference, in 1979 Zink attempted to use the result of experiments made in an electrolytic tank, to obtain an equation for a surface potential in the corner mesh. The difference is that he performed a regression analysis of the test data published in /13/, with respect to the IEEE simplified formula for E_{mesh} (17), trying to match the test data by means of a function of N (replacing the factor Ki in the formula), while retaining Km as valid. Because of this choice which substitutes a matching function of just one variable (N) for Ki, the product yields results on a high side, due to the shape of a regression curve. Also, since the very simple formula for ground resistance, eq. (37) is used to define the percent mesh voltage, the obtained expression cannot adequately reflect the effect of the depth of burial h. Column EMZIN in Tables 1-11 documents the performance of (56), obtained as follows: Defining the percent mesh potential in terms of GPR = Rg Io, and solving for Km Ki,

$$\frac{E_{mesh}}{R_g I_o} 100\% = \frac{200 K_m K_i}{2 + N \sqrt{\pi}} \approx 12.5 K_m + 83.3/N + 2.08 \tag{55}$$

results in

$$K_m K_i \approx (0.111 K_m + 0.0184) N + 0.125 K_m + 0.759 + 0.833/N \tag{56}$$

7. EFFECT OF CRUSHED-STONE LAYER ON ALLOWABLE SURFACE VOLTAGE

7.1 Evaluation of a Safe Touch Voltage Above a Grid

Once the critical surface potentials above a grounding grid are determined, it should be a simple task to decide if the design does or does not meet the requirements of IEEE 80. It is not. Incompatibility of principal assumptions makes it difficult to apply the required safety criteria correctly. For instance, Vx < V should assure compliance with a given safety rule; here, a surface voltage Vx to be less than the allowed value V.

However, in terms of the Guide, Vx not always is a true surface voltage with respect to V. On one hand, V by definition refers only to the surface material - no matter what may be below this surface. On the other hand, Vx is obtained by means of a simplified method which is based on the assumption of uniform soil. Therefore, Vx as such, is a voltage on the earth's surface, regardless if eventually a layer of protective material is put on the bare ground, or not. The significance of this circumstance is analyzed next.

The present Guide 80 defines the maximum allowable voltage for a touch type of contact, as

$$E_t \max = (R_b + \frac{1}{2} R_f) I_b(t). \tag{57}$$

In this expression, Rb represents the resistance of a human body equal to 1000 ohms, Ib(t) is the time-dependent limit of a non-fibrillating current through the body resulting from Dalziel's 99.5 % safety formula Ib = 0.116/ t, Ib in amps, t in seconds; and Rf is a combined resistance of two bare feet in contact with ground surface. This last term is calculated, in ohms, as equal to 1.5 |p|, where |p| denotes a numerical value of the surface material resistivity given in ohm-m. Using Laurent's formula for the resistance of a circular plate at zero depth, R = 0.25 p/r, it is easy to see that Rf represents the ground resistance of an equivalent metallic disc having approximately 16 cm in diameter: Rf becomes equal to 3 |p| for radius r = 0.083 m, if a uniform medium of resistivity p is assumed to infinite depth.

A question therefore arises, as how to correctly interpret (57), and how to estimate the effective value of Rf/2, if:

- a) the surface is covered by a relatively thin (4 - 5 inch) layer of gravel or similar material of a resistivity much higher than that of the soil, and
- b) the grounding grid is buried close to the ground surface.

7.2 An Equivalent Electrode Assumption

In order to analyze points a) and b) in simple terms, assume for a moment that the source of current is grounded far from the station, and just a single "foot" electrode represents both feet.

Choosing an equivalent hemisphere rather than a disc, its radius is $a = 1m/3\pi = 0.106$ m. In an unbounded volume of gravel of resistivity p , the apparent resistance of this electrode is:

$$R_a(p) = \frac{p}{2\pi} \int_a^\infty \frac{dx}{x^2} = \frac{p}{2\pi a} = 1.5 [p] \text{ for } a=0.106 \text{ m} \quad (58)$$

Since all equipotentials are concentric hemi-spheres, the integration can be viewed as a summation of a series of resistances: each resistance being that of a thin soil shell, and each consecutive shell having its diameter increased by dr .

7.3 Effect of a Thin Overlay

Consider now a layer of gravel of thickness h' , which is spread over a perfectly conductive earth. A current distribution on the the gravel-soil boundary is identical to the distribution found in a plane of symmetry between two sources of opposite polarity, with the sources set $2h'$ apart in a boundless medium. Because most of the current leaks down within a relatively limited area, Figure 12, the area which is covered by the gravel does not have to be very large, to be assumed of infinite size for a valid approximation.

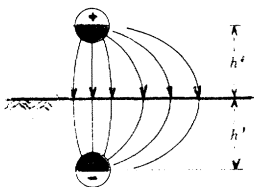


Figure 12.

Thus, using superposition, the electrode apparent resistance is:

$$R_a(p, h') = \frac{p}{2\pi} \left(\int_a^\infty \frac{dx}{x^2} - \int_{2h'-a}^\infty \frac{dx'}{x'^2} \right) = R_a(p) \left(1 - \frac{a}{2h'-a} \right) \quad (59)$$

This result can be interpreted as stating that for an equivalent hemisphere the effect of a surface layer of thickness h' is the same as if the hemisphere were coated with a $2h'$ layer of gravel forming a concentric shell. The following equation is a simple extension of this concept taken one step further, to account for a semi-infinite volume of soil surrounding the gravel. The soil has non-zero resistivity p_0 ; $0 < p_0 < p$.

Here,

$$R_a(p, p_0, h') = R_a(p, h') + \frac{p_0}{2\pi} \int_{2h'-a}^\infty \frac{dx'}{x'^2} = \frac{p}{2\pi a} C \quad (60)$$

An important implication of this formula is the fact that an effective value of R_f can be simply calculated by (58), if the resistivity of the surface material "p" is replaced by a derated resistivity $p' = pC$, using the factor C below.

$$C = 1 - a(1 - p_0/p)/(2h' - a) \quad (61)$$

7.4 Effect of Grid Proximity

The proximity of an energized grid has so far been neglected. In order to account for a set of conductors having a potential (E_0) which is higher than the potential at the point of a "foot" contact, the current lines which radiate from the "foot" electrode can be visualized as if these are being forced to spread wide in a limited space between the grid and the air-soil boundary. Such a behavior is analogous (and its cause is similar) to the effect of two parallel non-conducting planes separated by a distance H, shown in Figure 13.

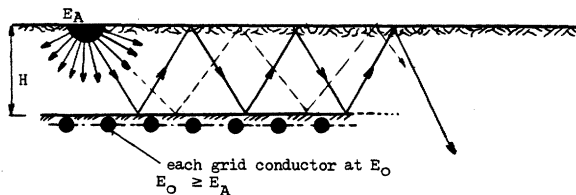


Figure 13.

As illustrated, a considerable number of the rays emerging from the "foot" hemisphere will change their direction at numerous reflection points, before entering the unobstructed space. And, albeit some adjustment will be necessary to accommodate the fact that only the air-earth plane is unbound, the basic formulation of this concept is an infinite reflection series.

Defining the apparent "foot" resistance as a function of H,

$$R_a(H) = \frac{p}{2\pi} \left(1/a + 2/x_1 + 2/x_2 + \dots + 2/x_n + \dots \right) \quad (62)$$

where

$$x_n = \sqrt{a^2 + (2nH)^2}$$

For $C=1$ and infinite H, $R_a(H)$ becomes R_a of (58):

$$R_a(H) = \frac{p}{2\pi} (1/a + 2/x_1 + 2/x_2 + \dots + 2/x_n + \dots) \quad (63)$$

$$\lim_{H \rightarrow \infty} R_a(H) = p/(2\pi a) = R_a(p)$$

A modification of the above equation to limit the effect of the lower plane, provides opportunity for several simplifications. First, for small a, such as $0 < a < 0.2$, all a^2 in (62) can be neglected, and the summation simplified. Let

$$\sum_{n=1}^{\infty} 1/x_n \approx \sum_{n=1}^{\infty} 1/2nH \approx S/H; \text{ series } S = \frac{1}{2} + \frac{1}{4} + \dots, n \rightarrow \infty. \quad (64)$$

In turn, the new series S can be replaced by a faster decaying series S^* , of which the infinite sum is known. Choosing S^* , as

$$S^* = \sum_{k=2}^{\infty} 1/k^2 = 1/4 + 1/9 + 1/16 + \dots, k \rightarrow \infty \quad (65)$$

$$S^* = 1.644934 - 1 \approx 0.65$$

the substitution of twice the infinite sum of S^* for $2S$, means:

$$2S \approx 1/2 + 2/9 + 1/8 + \dots \approx 1.3 \quad (66)$$

A relatively simple equation for the apparent resistance of an equivalent "foot" electrode in the presence of a grid, emerges as a result of applying (66) and (64) to (62):

$$R_a^*(H) = \frac{p}{2\pi a} (1 + 1.3 a/H); \quad \sigma = pC \quad (67)$$

Alternatively, in a notation which is consistent with (59) and (60), the formula can be expressed as:

$$R_a(p, p_0, h', h) = R_a(p) C (1 + 1.3a/(h+h')) \quad (68)$$

where in addition to the already established symbols, h is depth of the grid burial; $H = h + h'$.

7.5 Known Test Case for Two Wires and Crushed-Stone Overlay

In the closure of Ref.(16), the following example was thoroughly analyzed with the use of a computer: Two counterpoise wires are buried in a 250 ohm-m soil which is covered by a 0.25 m layer of crushed stone, having an average resistivity of 5,000 ohm-m. The wires are placed 0.5 m below the soil surface, and spaced 10 m apart. Each wire has a 0.014 m diameter (1/0 AWG size). Assuming a man standing atop the protective layer and touching a grounded object above a centerline between the wires, the value of an apparent resistance of his feet was determined to be 6,447 ohms. The corresponding value of derated crushed-stone resistivity, is 75 % of a nominal value, i.e. $C = 0.75$.

Alternatively, this particular value of 0.75 was further checked against another value, obtained from a general set of derating curves which have been proposed for such a purpose in Ref. (25). Reading of a $C(K, h)$ curve for $K = -0.9$ and for $h = 0.25$ m, produced a 0.82 value for the derating factor; $K = (p_0 - p)/(p_0 + p)$.

In view of these results, the outcome of using (61) and (68) may be of interest:

If the effect of counterpoise wires is neglected, (61) applies; substitution of $p = 5,000$ ohm-m, $p_0 = 250$ ohm, and $h' = 0.25$ m, gives

$$C = 1 - 0.106(1 - 250/5000)/(0.5 - 0.106) = 0.7441$$

$$R_a(5000, 250, .25) = 1.5 \times 5000 \times C = 5581 \text{ ohms}$$

If the two wires are viewed as a grid, and equation (58) is applied (using the already known result for the derated resistivity pC , and the depth parameter $H = 0.75$ m), the result is:

$$R_a^*(0.75) = 5581 \times (1 + 1.3(0.106/0.75)) = 6607 \text{ ohms}$$

$$(6607 \text{ ohms}/5581 \text{ ohms}) \times 0.7441 = 0.881$$

So, with no grounding conductor near the point of feet contact, the derating factor is equal to 0.744. With the "grid" 0.75 m distant from the ground surface, the effective derating is 0.88. Of course, the geometry of two counterpoise wires hardly justifies the use of the second method of calculation. Generally, if a grid is buried near the surface, the apparent "foot" resistance may approach $1.5 |p|$. In the example, this condition would occur for $H = 0.4$ m, i. e. for a grid buried in a 0.15 m depth.

8. RECOMMENDATIONS FOR ESTIMATING E_{mesh}

Although the new equations (41) and (42) have been tested in a design series which included up to 48 subdivisions of the basic one-mesh grid, it is felt that the simplified method should not be used for grids with more than 225 meshes ($N=16$), since a 900 mesh grid design ($N=31$) probably is the utmost end of the theoretically acceptable range of N values. Thus, using an average,

$$N < 25 \text{ is suggested as a limit.}$$

The other recommended constraints are: $0.25 \text{ m} < h < 2.5 \text{ m}$
 $d < 0.25 h$; $D > 2.5 \text{ m}$

2.5 : 1 maximum length-to-width ratio for rectangular grids

Generally, the new equations can be applied to those rectangular grids which can be visualized as a "stretched square", that is, having identical number of conductors in the north-south and in the east-west direction. Since the first formula has been linked to the concept of a grid-rod design utilizing ground rods only along the perimeter, while the second one applies to the remaining alternatives of using a grid with ground rods which are predominantly placed inside the grid area, or with no rods at all, these equations determine the probable range of the mesh voltage values which can be expected for most designs in practice.

9. CONCLUSIONS

9.1 Summary of Part I

- Fundamental characteristics of the basic mathematical model of the IEEE gradient method have been evaluated and the difficulties experienced in the past with the simplified formula for E_{mesh} , explained.
- New simplified equations for E_{mesh} , based on a symmetrical model of a corner mesh, have been developed and tested. The limits of applicability have also been established.
- In addition, simple expressions for estimating the grounding resistance, and for derating of the nominal resistivity of a thin surface layer of a highly-resistive material near or above a grounding grid, have been provided.

9.2 Closing Remarks

It should be born in mind that the method yields good estimates, at best. Of course, the whole pre-occupation with a corner mesh results just from one crucial decision: to use an equally spaced grid. Once this concept is abandoned, the whole approach to designing a safe grounding grid can and will be changed. As it is apparent from Figure 14 below, and as it will be explored in the following paper, Part II, the corner mesh no longer will be much of a problem.

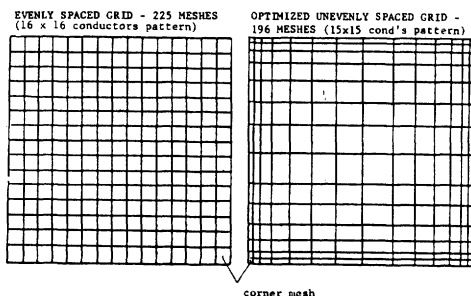


Figure 14.

9.3 How Good is This Method?

After accounting for the inherent limitations of the basic model, quite good, actually.

Acknowledgement

Thanks are expressed to Dr. Dawalibi of SES Ltd., Montreal, for making computer runs with program MALT, for the examples specified in paragraph 5.3, to demonstrate the influence of ground rods. Program MALT Version 2, Rev.6, was used in November 1979.

Figure 2 was obtained during the development of program RENA 3, a later version of program RENA described in 77, of the United Engineers and Constructors Inc., Philadelphia. All other computer calculations were done on the computer facilities of Gibbs & Hill, Inc., New York.

REFERENCES

- /1/ AIEE Committee Report "Voltage Gradients Through the Ground Under Fault Conditions", F. Stevens chmn., AIEE Trans. Vol. PAS-77, pp. 669-692, October 1958.
- /2/ AIEE No. 80 / March 1961, GUIDE FOR SAFETY IN A-C CURRENT SUBSTATION GROUNDING, by American Institute of Electrical and Electronics Engineers, New York, 1961.
- /3/ IEEE Std. 80 / June 1976, IEEE GUIDE FOR SAFETY IN SUBSTATION GROUNDING, by Institute of Electrical and Electronics Engineers, New York, 1976.
- /4/ F. Dawalibi, M. Bouchard and D. Mukhedkar, "Survey on Power System Design Practices", IEEE Trans. Vol. PAS-99, No.4, pp. 1396-1405, July-August 1980.

- /5/ E.T.B. Gross, B. V. Chitnis, and L. J. Stratton, "Grounding Grids for High Voltage Stations", AIEE Trans., Vol. PAS-72, pp. 799-810, August 1953.
- /6/ F. Dawalibi and D. Mukhedkar, "Optimum Design of Substation Grounding in Two-Layer Earth Structure, Part I - Analytical Study", Ibid., Vol. PAS-94, No.2, pp. 252-261, March-April 1975.
- /7/ J. G. Sverak, "Optimized Grounding Grid Design Using Variable Spacing Technique", IEEE Trans., Vol. PAS-95, No. 1, pp. 362-374, January/February 1976.
- /8/ L. G. Zukerman, "Simplified Analysis of Rectangular Grounding Grids", Ibid., Vol. PAS-98, No. 5, pp. 1777-1787, Sept./Oct. 1979.
- /9/ L. E. Craford, M. S. Griffith, "A Closer Look At The Facts Of Life In Ground Mat Design", IEEE Transact. on Industry Applications, Vol. IA-15, No. 3, pp. 241-250, May-June 1979.
- /10/ J. Nahman and S. Skuletich, "Irregularity Correction Factors for Mesh and Step Voltages of Grounding Grids", IEEE Trans., Vol. PAS-99, No. 1, pp. 174-180, Jan./Feb. 1980.
- /11/ J. Nahman and S. Skuletich, "Resistances to Ground and Mesh Voltages of Ground Grids", Proc. IEE, Vol. 126, No. 1, pp. 57-61, January 1979.
- /12/ W. Koch, "Erdungsmaßnahmen für Hochspannungsanlagen mit Geerdetem Sternpunkt", Elektrotechnische Zeitschrift, Vol. 71, No.4, pp. 89-91, February 1950.
- /13/ B. Ithapar and K. K. Puri, "Mesh Potentials In High Voltage Grounding Grids", IEEE Trans. Vol. PAS-86, No.2, pp.249-254, February 1967.
- /14/ R. G. Harrington, "Matrix Methods for Field Problems", Proc. of the IEEE, Vol. 55, No. 2, pp.136-149, February 1967.
- /15/ P. Koutevnikoff, "Numerical Computation of The Grounding Resistance of Substations and Towers", IEEE Trans., Vol. PAS-99, No.3, pp. 957-965, May/June 1980.
- /15a/ Discussion of (15) by A.P. Meliopoulos, R.P. Webb, and E. B. Joy, Ibid., pp. 963-964.
- /16/ R. J. Heppie "Step Potentials And Body Currents Near Grounds Grounds In Two-Layer Earth", Ibid., Vol. PAS-98, No. 1, pp. 45-59, January-February 1979.
- /17/ R. J. Heppie, "Computation of Potential at Surface Above An energized Grid or Other Electrode, Allowing for Non-Uniform Current Distribution", Ibid., Vol. PAS-98, No. 6, pp. 1978-1988, November-December 1979.
- /18/ B. Ithapar and R. P. Nagar, "Irregularity Correction Factor For Grounding Grids", Journal of Institution of Engineers, (India), Vol. 58, Pt. EI-1, pp.36-41, August 1977.
- /19/ J. H. Zink, "Comments On The IEEE Guide No. 80 for Safety In Substation Grounding", IEEE Conference Paper A-79-549-7, 1979.
- /20/ F. Dawalibi and D. Mukhedkar, "Influence Of Ground Rods On Grounding Grids", IEEE Transactions, Vol. PAS-98, No. 6, pp. 2089-2097, Nov./Dec. 1979.
- /21/ A. Voronina, "Naprazhenija Prikosnovenija I Potencial Sloznych Zazemlitatej v Odnorodnoj Zemlje", Elektricitstvo (USSR) No. 7, pp. 52-56, July 1969.
- /22/ S. J. Schwarz, "Analytical Expressions for the Resistance of Grounding Systems", AIEE Trans., Vol. PAS-73, pp. 801 - 809, October 1955.
- /23/ E.T.B. Gross, and R. S. Hollich, "Grounding Grids for High Voltage Stations III -- Resistance of Rectangular Grids", AIEE Trans., Vol. 75, pp. 926-935, October 1956.
- /24/ H. R. Armstrong and L. J. Simpkin, "Grounding Electrode Potential Gradients from Model Tests", AIEE Trans. Vol. 79, No. 5, pp. 618-622, October 1960.
- /25/ J. G. Sverak, W. K. Dick, T. H. Dodds, and R. H. Heppie, "Safe Substation Grounding, Part I", IEEE Working Group 78.1 Report IEEE Trans. Vol. PAS-100, pp. 4281-4290, September 1981.
- /26/ J. G. Sverak et al., "Safe Substation Grounding - Part II", IEEE Working Group 78.1 Report, Ibid., Vol. PAS-101, No. 10, pp. 4006-4023, October 1982.

APPENDIX I - Analysis Of Gradient Problem; Basic Mathematical Model

Generally, in a boundless homogeneous medium of resistivity σ , the voltage difference between two points X_1 and X_2 at a respective distance r_1 and r_2 from a line source dissipating current i per unit length, is:

$$E_{12} = \frac{di}{2\pi} \int_{r_1}^{r_2} (1/r) dr = \frac{di}{2\pi} \ln (r_2/r_1) \quad (I-1)$$

If the line source is buried in shallow depth h below a flat ground surface, and the points X_1 and X_2 are both placed on the surface, the voltage difference between them can be calculated as if it is caused by wire (1) in depth h , and by a mirror image of the wire (1*) placed symmetrically in a distance $-h$ above the ground plane; assuming now again the medium σ as filling the entire space. Figure 15.

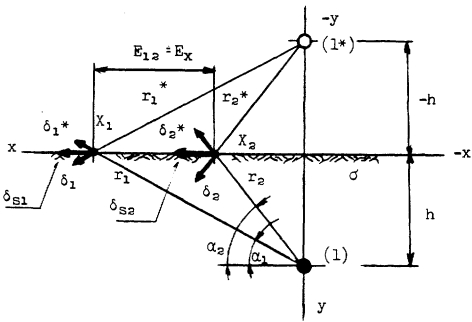


Figure 15.

From the geometry of Figure 15 is apparent that at any point $X(x,0)$ on the surface, (here $X = X_i$, $i = 1,2$), the surface current density per unit area δ_s due to current i flowing both from the wire (1) and the wire image (1*) is, as a vector in space,

$$\delta_s = \frac{i}{2\pi r} (\cos \alpha + j \sin \alpha) + \frac{i}{2\pi r^*} (\cos \alpha - j \sin \alpha) \quad (I-2)$$

where α is angle between the direction of the current δ and the horizontal plane.

Since $\text{Abs.}(r) = \text{Abs.}(r^*) = (x^2 + h^2)^{\frac{1}{2}}$, and $\cos \alpha = x/r$, $\sin \alpha = y/r$,

it follows that

$$\delta_s = \frac{i}{2\pi r} (2 \cos \alpha) = \frac{i}{\pi} \frac{x}{x^2 + h^2} \quad (I-3)$$

The voltage difference between points X_1 and X_2 , as a scalar, is:

$$E_x = \int_{X_1}^{X_2} \delta_s ds = \frac{\sigma i}{\pi} \int_{x_1}^{x_2} \frac{x dx}{x^2 + h^2} = \frac{1}{2\pi} \sigma i \ln \left[\frac{x_2^2 + h^2}{x_1^2 + h^2} \right] \quad (I-4)$$

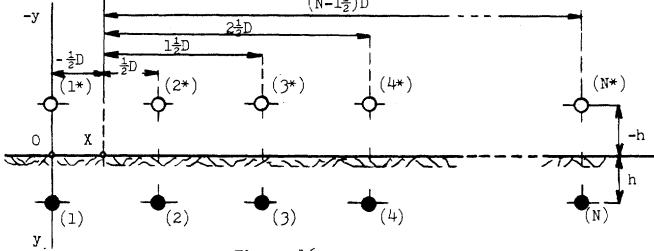


Figure 16.

Consider now a set of N equally spaced parallel wires and their images, as shown in Figure 16 above. Here the distance between two given points on the earth's surface, $O(0,0)$ and $X(-\frac{1}{2}D,0)$, is $\frac{1}{2}D$, and the distance between any two line sources is D . With such a geometry, the difference in the surface potentials from O to X , produced by k -th wire and its image, can be expressed as

$$E_x(k) = \frac{\sigma i}{\pi} \int_{-\frac{1}{2}D}^{\frac{1}{2}D} \frac{x(k) dx}{x(k)^2 + h^2}; \quad x(k) = (k-1)D + x; \quad k = 1,2, \dots \quad (I-5)$$

If the assumption is made that the electrical field of an individual wire is not affected by the presence of other wires, then the effect of N line sources and N images on the resulting voltage between O and X , is a sum of the individual contributions determined by superposition, wire by wire:

$$E_x = \sum_{k=1}^N E_x(k) = \sigma i K_{mx}(1,N) = \sigma i \sum_{k=1}^N \frac{1}{2\pi} \ln \left[\frac{[(k-\frac{1}{2})D]^2 + h^2}{[(k-1)D]^2 + h^2} \right] \quad (I-6)$$

Alternatively, the factor $K_{mx}(1,N)$ which represents this effect of N wires on the surface voltage m_x along x -axis, (from the position above the first wire toward the point above the centerline between the first and the second wire), can be stated as:

$$K_{mx}(1,N) = \frac{1}{2\pi} \sum_{k=1}^{N-1} \ln \left[\frac{4h^2 + (2k-1)^2 D^2}{4h^2 + 4(kD)^2} \right] \quad (I-7)$$

Although the potential difference between O and X has been obtained by (I-6), their potential with respect to a remote ground remains unknown and has to be determined. If all N wires and their images are assumed to be at potential E_0 during a ground fault, so that

$$E_0 = R_0 I_0; \quad \text{where } R_0 \text{ is the grounding system resistance} \quad (I-8)$$

I_0 is the total current flowing into ground, i.e. $I_0 = i \times L$, L being the total length of buried wires;

the voltage at point O , produced by the first conductor and its image, is:

$$V_0(1) = E_0 - E_y(1) \quad (I-9)$$

Here, using (I-1) and integrating from the surface of both the real and the image line source to the point O on the air-earth boundary, $E_y(1)$ is calculated as follows:

$$E_y(1) = \frac{1}{2\pi} \sigma i \left[\int_{\frac{1}{2}d}^h \frac{1}{y} dy + \int_{\frac{1}{2}d}^h \frac{1}{2h-\frac{1}{2}d} \frac{1}{y^*} dy^* \right] \quad (I-10)$$

which can be expressed under one integral, as

$$E_y(1) = \frac{\sigma i}{2\pi} \int_{\frac{1}{2}d}^h \left(\frac{1}{y} - \frac{1}{2h-y} \right) dy = \frac{\sigma i}{2\pi} \left[\ln \left(\frac{2h}{d} \right) + \ln \left(\frac{2h}{4h-d} \right) \right], \text{ or}$$

$$E_y(1) = \frac{\sigma i}{2\pi} \ln \left[\frac{4h^2}{4hd - d^2} \right]. \quad (I-11)$$

Similarly as before, the voltage at point O produced by any other wire than the first one, generally is

$$V_0(k) = E_0 - E_y(k); \quad k = 2,3, \dots, N \quad (I-12)$$

Using (I-1) again, once for the real source and once for its image, the general form of $E_y(k)$ can be written as

$$E_y(k) = C \int \frac{1}{r_k} dr + C \int \frac{1}{r_k^*} dr^* \quad (I-13)$$

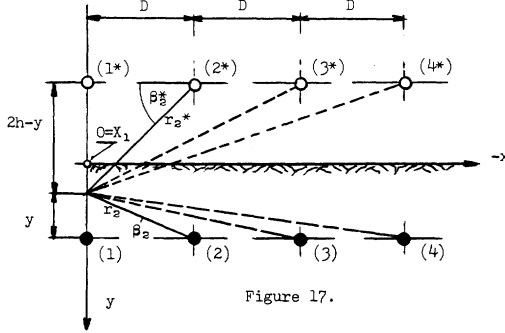


Figure 17.

Based on the geometry of Figure 17 above, it can be seen that for a vertical voltage drop the following substitutions hold for all k 's, including $k = 1$:

$$r_k = \sqrt{y^2 + (k-1)^2 D^2}; \quad dy = dr \sin \beta_k = y dy/r_k; \quad C = \frac{\sigma i}{2\pi} \quad (I-14)$$

$$r_k^* = \sqrt{(2h-y)^2 + (k-1)^2 D^2}; \quad dy = -dr^* \sin \beta_k^* = (y-2h)dy/r_k^* \quad (I-15)$$

so that the integral solution for $E_y(k)$ becomes

$$E_y(k) = \frac{\sigma i}{2\pi} \int_{\frac{1}{2}d}^h \frac{y dy}{y^2 + (k-1)^2 D^2} + \frac{\sigma i}{2\pi} \int_{\frac{1}{2}d}^h \frac{(y-2h) dy}{(2h-y)^2 + (k-1)^2 D^2} \quad (I-16)$$

$$= \frac{\sigma i}{4\pi} \ln \left[\frac{(k-1)^2 D^2 + h^2}{(k-1)^2 D^2 + \frac{1}{4}d^2} \right] \cdot \left[\frac{(k-1)^2 D^2 + h^2}{(k-1)^2 D^2 + (2h-\frac{1}{2}d)^2} \right]$$

By superposition, the voltage at point O due to the effect of N real and N imaginary line sources, is:

$$V_0 = E_0 - \sum_{k=1}^N E_y(k) = E_0 - \sigma i K_{my}(1,N) = E_0 - E_y; \quad E_y = \sum_{k=1}^N E_y(k) \quad (I-17)$$

where

$$K_{my}(1,N) = \frac{1}{4\pi} \sum_{k=1}^{N-1} \ln \left[\frac{(kD)^2 + h^2}{(kD)^2 + \frac{1}{4}d^2} \cdot \frac{(kD)^2 + h^2}{(kD)^2 + (2h-\frac{1}{2}d)^2} \right] \quad (I-18)$$

Now the voltage at point X can also be determined; referring to (I-6), it follows

$$V_X = E_0 - (E_x + E_y) = E_0 - \sigma i (K_{mx}(1,N) + K_{my}(1,N)) \quad (I-19)$$

Finally, since the potential of all grounded structures is E_0 , the touch voltage in the center of the "corner mesh", is:

$$V_t = E_0 - V_X = E_x + E_y \quad (I-20)$$

APPENDIX II - Derivation of Mesh Factor K_m for $N = 2$ and $h \geq 4d$

Based on the analysis of the basic model in Appendix I, for $N = 2$ the mesh voltage factor can be expressed in terms of its x -components and y -components, wire by wire, as

$$K_m = K_{mx}(1,2) + K_{my}(1,2) = K_{mx}(1) + K_{mx}(2) + K_{my}(1) + K_{my}(2) \quad (II-1)$$

where

$$K_{mx}(1) = \frac{1}{2\pi} \ln \left[\frac{(4h^2 + D^2)}{(4h^2)} \right] \quad (II-2)$$

$$K_{mx}(2) = \frac{1}{2\pi} \ln \left[\frac{(4h^2 + D^2)}{(4h^2 + 4d^2)} \right] \quad (II-3)$$

$$K_{my}(1) = \frac{1}{2\pi} \ln [(4h^2)/(4hd - d^2)] \quad (II-4)$$

$$K_{my}(2) = \frac{1}{4\pi} \ln [(h^2+d^2)/(D^2 + \frac{1}{4}d^2)] + \frac{1}{4\pi} \ln [(h^2+d^2)/(D^2 + (2h - \frac{1}{2}d)^2)] \quad (II-5)$$

Combining (II-2) and (II-4) and simplifying for small d and $h \geq 4d$, by neglecting all $\frac{1}{4}d$ and $\frac{1}{4}d^2$ terms, one gets

$$K_{mx}(1) + K_{my}(1) \approx \frac{1}{2\pi} \ln [(1 + D^2/4h^2)(4h^2/(4hd - 0))] \approx \frac{1}{2\pi} \ln [(h/d) + (D^2/4hd)] \quad (II-6)$$

and similarly, for (II-3) and (II-5), using a square of (II-5),

$$K_{mx}(2) + K_{my}(2) \approx \frac{1}{4\pi} \ln [[(4h^2+d^2)/(4h^2+4D^2)]^2] + \frac{1}{4\pi} \ln [(h^2+d^2)/[(D^2+0)(D^2+(2h-0)^2)]]$$

which, after some manipulation and multiplying of arguments, gives

$$K_{mx}(2) + K_{my}(2) \approx \frac{1}{2\pi} \ln (\frac{1}{4} + h/2D). \quad (II-7)$$

Denoting formally the simplified expressions (II-6) and (II-7), as $K'_{mxy}(1)$ and $K'_{mxy}(2)$, it holds

$$K'_{mxy}(1) + K'_{mxy}(2) = \frac{1}{2\pi} \ln [(h/d)(1 + D^2/4h^2)(\frac{1}{4} + h/2D)] \quad (II-8)$$

Since the order in which the individual members of (II-1) are summed does not matter, obviously

$$K'_{mx}(1,2) + K'_{my}(1,2) = K'_{mxy}(1) + K'_{mxy}(2) \quad (II-9)$$

and the mesh factor for $N = 2$ and $h \geq 4d$, is approximately

$$K_m(N=2) \approx \frac{1}{2\pi} \ln \left[\frac{D^2}{16hd} + \frac{(D+2h)^2}{8Dd} - \frac{h}{4d} \right] \quad (II-10)$$

APPENDIX III - Numerical Approximation of $K'_{mx}(3,N)$ Series for $h \rightarrow 0$

For N parallel conductors representing a grounding grid, the mesh voltage factor K_m can be viewed as consisting of three components:

$$K_m = K'_{my}(1,2) + K'_{mx}(1,2) + K'_{mx}(3,N) \quad (III-1)$$

where in particular, for a zero burial depth,

$$K'_{mx}(3,N) = (1/\pi) \ln [(3/4)(5/6)(7/8) \dots] \quad (III-2)$$

reflects the beneficial effect of $(N-2)$ parallel conductors outside the "corner mesh" on lowering the voltage difference between the voltage on grounded metal and that existing on the earth's surface, above a center line between the first two peripheral conductors forming the first mesh.

Thus,

$$K'_{mx}(3,N) = \frac{1}{\pi} \sum_{k=1}^{n=N-2} \ln (a_k) = (1/\pi) \ln (S_N) \quad (III-3)$$

where

$$S_N = \prod_{K=3}^N \left[\frac{2K-3}{2K-2} \right] \quad (III-4)$$

Since

$$\lim_{n \rightarrow \infty} (a_n) = 1, \text{ and } 0.75 \leq a_k < a_{k+1} < 1, \text{ for } k = 1, 2, \dots$$

$K'_{mx}(3,N)$ is subtractive; the higher N , the higher negative value of the logarithm of S_N results.

Consequently, in order to approximate the series by a simple function, and to keep errors sufficiently small and on the conservative side, we will seek such a functional S_N^* , which will satisfy the following conditions:

- a) $S_N^* = \sup \{ S_N \}$ for any $N \in (3 \leq N < \infty)$ (III-5)
- b) $\lim_{N \rightarrow \infty} (S_N^* - S_N) = +0$ (III-6)

and, for any countably finite series, such a small positive error margin δ , $\delta \geq 0$, which will be acceptable. To prevent runaway errors for high N , this last requirement represents the need for a convergence; that is for any small positive number $\gamma \leq \delta$, there always exists a positive integer I such, that

$$c) (S_K^* - S_K) \leq \gamma \text{ for } K \in (3, N + I). \quad (III-7)$$

Consider now the following two double factorials:

$$(2n-1)!! = (2n-1)(2n-3)(2n-5) \dots 5 \cdot 3 \cdot 1$$

$$(2n)!! = (2n)(2n-2)(2n-4) \dots 6 \cdot 4 \cdot 2$$

Let

$$S_n = \frac{(2n-1)!!}{(2n)!!} \quad (III-8)$$

Comparing (III-4) and (III-8), it can be seen that for $n = N - 1$,

$$S_n = \frac{[(2N-3)!!]}{[(2N-2)!!]} = (\frac{1}{2}) S_N \quad (III-9)$$

As shown in mathematical handbooks, $\pi/2$ can be represented by the following infinite series:

$$\frac{1}{2}\pi = (2)(2/3)(4/3)(4/5)(6/5)(6/7)(8/7)(8/9) \dots \quad (III-10)$$

A closer analysis of (III-10) reveals that a very useful relationship exists between the number π and S_n , as defined in (III-8):

$$\lim_{n \rightarrow \infty} \left\{ \left[\frac{(2n-1)!!}{(2n)!!} \right]^2 (2n+1) \right\} = 2/\pi \quad (III-11)$$

Using (III-9), it is easy to see that, furthermore,

$$2/\pi = \lim_{n \rightarrow \infty} [(2n+1)(S_n)^2] = \lim_{N \rightarrow \infty} [(2N-1)(S_N/2)^2] \quad (III-12)$$

On this basis, for any countable finite series S_N , $N \in (3 \leq N < \infty)$, the following inequality holds:

$$(2N-1)(S_N)^2 \geq 8/\pi, \text{ or } S_N \geq (8/\pi(2N-1))^{1/2} \quad (III-13)$$

Therefore, the sought functional S_N^* , is:

$$S_N^* = \sqrt{\frac{8}{\pi(2N-1)}} \quad (III-14)$$

Proof: Expressing S_n by means of a gamma function $\Gamma(x)$ for the particular x ; $x = n+1$, and $x = n+\frac{1}{2}$ values,

$$\Gamma(n+1) = n! \text{ and } \Gamma(n+\frac{1}{2}) = \frac{(2n)! \sqrt{\pi}}{n! 2^{2n}}$$

Thus,

$$S_n = \frac{(2n-1)!!}{(2n)!!} = \frac{2^n \Gamma(n+\frac{1}{2})}{\sqrt{\pi}} \cdot \frac{1}{2^n \Gamma(n+1)}$$

$$= \frac{(2n)!}{2^{2n} (n!)^2} \quad (III-15)$$

Substitution of (III-15) into (III-12) yields:

$$2/\pi = \lim_{n \rightarrow \infty} \left\{ (2n+1) \left[\frac{(2n)!}{2^{2n} (n!)^2} \right]^2 \right\} \quad (III-16)$$

Now, consider two integers: μ , and ν , ($1 < \mu < \nu < n < \infty$), say, $\mu = 5$, $\nu = 7$, and let $n = 25$.

Then,

$$S_{(5)} > S_{(7)} > S_{n=25} > 2/\pi \text{ should hold.}$$

Provide

$$11(10!/(2^{10}(5!)^2))^2 > 15(14!/(2^{14}(7!)^2))^2 > 51(50!/(2^{50}(25!)^2))^2 > 2/\pi.$$

Calculated,

$$0.66618 > 0.65818 > 0.64289 > 2/\pi \approx 0.63662$$

or, more vividly,

$$2/0.9556\pi > 2/0.9672\pi > 2/0.9902\pi > 2/\pi.$$

Hence, $K'_{mx}(3,N)$ can be approximated with reasonable accuracy, as

$$K'_{mx}(3,N) = \frac{1}{\pi} \ln \left[\sqrt{\frac{8}{(2N-1)\pi}} \right] \quad (III-17)$$

$$= (1/2\pi) \ln (8/(\pi(2N-1)))$$

Discussion

David W. Jackson (Chas. T. Main, Inc., Engineers, Boston, MA): This is excellent work, full of thoughtful insight, and quite clearly presented. It is comprehensive and timely.

The simplified method based on IEEE 80 has much to recommend. It lends to application of desk top and programmable calculators for solution of a range of ground grids, from small industrial substations to large utility stations.

Section 7.3 of the paper contains an error. The correction factor (equation 59), $C = (1-a/(2h-a))$ cannot hold for thin top layers of h thickness, where $0 < h < 3a$. There is no disagreement with the multiplication of the second term of the correction factor (after correcting as discussed below) by $(1 - \rho_0/\rho)$, where the base strata has a non-zero resistivity.

It is useful to assume zero resistivity for the under layer. The basic foot contact resistance is $R = 1.5 \rho$, for which is used either the Laurent disc simplification of $R = \rho/4r$, where $r = 1/6$, or a hemispherical equivalent electrode $R = \rho/2\pi a$ where $a = 1/3 \pi$. Examine the behavior of the correction term $(1-a/(2h-a))$ for values of h between 0 and $3a$; see Col. 1 of Table 1. For variations in thickness of thin layers one would expect a continuous increase in resistance R from $h=0$, approximately linearly up till $h=a$. Proposed equation 59 correction factor varies from zero at $h=a$ to minus infinity at $h=a/2$, to 2 at $h=0$.

In section 7.3 it is stated that for an equivalent hemispherical electrode this result can be interpreted as the effect of a $2h$ thick layer of gravel enveloping the hemisphere. I disagree. It does not act that way. In fact it responds as though it were a hemisphere pressed into a thin layer, and when $h=a$ so that the hemisphere just touches the zero resistivity layer beneath, R becomes zero.

It might appear that this anomaly stems from the assumption of an equivalent hemisphere. Consider the assumption of equivalent Laurent disc electrodes in homogenous medium separated by distance $2h$. The integration distance becomes $2h$. The basic foot contact resistance becomes $1.5 \rho = \rho/4r$. The correction factor C_1 becomes $(1-r/2h)$ where $r = 1/6$. However, C_1 does not behave reasonably for thin layers. See Col. 2 of Table 1. C_1 goes to zero at $h=r/2$, and to minus infinity at $h=0$.

The form of the correction factor C , reveals that the second term must have a positive "a" in the denominator to cause the factor to go to zero at $h=0$. Return to the statement that the equivalent hemisphere did (or should) behave as though wrapped in a $2h$ thick layer. Assume this, and calculate the resistance of the layer $2h$; where $R = \rho \int_A \frac{1}{A} = \rho \int \frac{dr}{2\pi r^2}$ between the limits of a and $a + 2h$. The correction factor becomes $C_2 = (1-a/(2h + a))$.

Behavior of C_2 for thin layers is shown in Col. 3 of Table 1. Its behavior is reasonable and satisfactory. One might hope for linear behavior when h is quite thin. Col. 3 shows that for values of h which are small fractions of a , that C_2 does vary approximately linearly.

I suggest that correction factor $C_2 = (1-a/(2h + a))$ is an accurate representation of foot contact resistance for thin top layers of thickness between zero and twelve inches. For thicker layers, $C = (1-a/(2h - a))$ would be a more accurate representation since it correctly reflects the current distribution in an appreciably thick layer.

TABLE 1

h	Approx Inches	Col. 1 $C = 1 - a / (2h - a)$	Col 2 $C = 1 - r / 2h$	Col. 3 $C_2 = 1 - a / (2h + a)$
0	0	2	$-\infty$	0
a/4	1	3		1/3
a/2	2	$-\infty$		1/2
3a/4	3	-1		3/5
a	4	0		2/3
1.5a	6	1/2		3/4
2a	8	2/3		4/5
3a	12	4/5		6/7
10.5a	42	19/20	21/22	
r/4	1.5			-1
r/2	3			0
r	6			1/2
1.5r	9			2/3
2r	12			3/4
a/100				.0196
2a/100				.0385
3a/100				.0566

Manuscript received June 13, 1983.

Eldon J. Rogers (Bonneville Power Administration, Vancouver, WA): The IEEE Standard 80-1961 since its publication has made an outstanding contribution to the understanding and precepts of safe grounding. Its summary of significant articles and the inclusion of premier papers (which are still referenced today) makes available, generally, the bulk of specialized grounding knowledge. Because of wide acceptance and successful application of the guide, the author is to be congratulated on his efforts which improve the accuracy and extend the range of guide's simplified formulas.

The author's ground rod example shows with a 24.6 percent increase in conductor length, corner mesh potential decreased 38 percent and grid resistance decreased 10 percent. What effect does perimeter rods have on external touch and step potentials? Larger grids would require the installation of longer rods. For the same increase in conductor length it would appear to be more economical to install horizontal wires along the perimeter to reduce mesh potential. Has the author established a relationship between rod length, number of rods and grid width? The author's example establishes the minimal effect ground rods have on reducing grid resistance. However, in addition to penetration of lower resistivity earth, the role of the ground rod is to provide impedance reduction and redundancy at equipment, arrestors and critical ground points.

Extremely accurate grid design is hampered by resistivity variations of the earth in contact with grid conductors that in many cases have variations as high as 4 to 1 across the grid. As a consequence, current density (A/m) and maximum touch and step will differ from those calculated by average values. Also, it has been our experience that the resistivity value used to calculate grid resistance differ from top earth resistivity and relates more to the deeper earth resistivity.

In addition to less simplifying assumptions, the author modifies $K_{mx}(3,N)$ with $H_m(h,h_0)$. How was H_m determined? Should the H_m factor be used to make "Et", Equation (67) page 38 reference [2] more accurate? If so, would the author include his modified equation for "Et" in his closure? Equation (41) and (42) are the finalized equation for mesh voltage. Have they been confirmed by computer or model testing?

Manuscript received March 1, 1983.

J. Nahman (University of Belgrade, Belgrade, Yugoslavia): The author has to be highly commended for deriving new formulas for grid mesh voltages taking into account more properly the actual geometry of the ground grid model under consideration. Since based upon a clear physical concept of the problem, the formulas mentioned can be expected to provide good estimates of grid mesh voltages in the most practical cases.

We would like to supply some information concerning the applicability of the approximate formulas for mesh voltages.

The expressions (52) and (54) have been constructed empirically to match the data obtained using complete computer grid modeling for square and rectangular grids up to 64 meshes ($N \leq 9$). Formula (54) has been also tested with experimental data reported in [13]. As evident from Table I and II, (54) gives results close to EMNEW1 and EMNEW2 also at higher N values, especially for $h = 2.5$ m. It is interesting to notice that, if a square plate is modelled as a round plate with the same A and h , the following mesh voltages for the plate are obtained: 66V for $h = 0.25$ m and 156V for $h = 2.5$ m. The mesh voltages of the plate are calculated at earth surface points above the plate edge.

Formula (54) has been used for assessing the mesh voltages for two 400 kV substations under construction in Yugoslavia, with ground grids lacking the ideal symmetry (Fig. D1 and Fig. D2). For both grids:

$h=0.7$ m and $d=0.01$ m. Taking $D=\sqrt{A/Nm}$ and $N=\sqrt{Nm} + 1$ with Nm being the number of grid meshes, the results are obtained listed in Table DI. Values $I_0=10$ kA and $\sigma=100$ Ω m have been assumed.

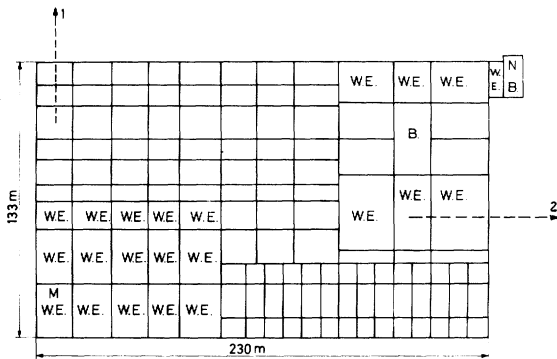


Fig. D1 400 kV-Titograd Substation ground grid
B-building WE.-without equipment

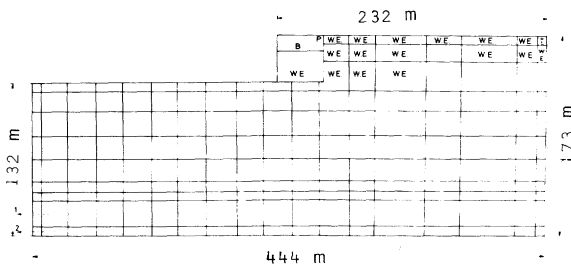


Fig. D2 400 kV-Mladost Substation ground grid
B-building WE.-without equipment

Table DI

Substation	Titograd			Mladost		
	complete computer modeling	Formula (54)	Error %	complete computer modeling	Formula (54)	Error %
Emesh, V	518	629	21	329	414	26

For the Titograd Substation Emesh values have been analyzed along lines 1 and 2 (Fig. D1). The highest value, given in Table DI, has been found on line 1 at the corner mesh. Higher Emesh values could be obtained at meshed M or N, but they are of no practical significance. Mesh M has no exposed grounded objects and mesh N surrounds the building the foundation of which considerably improves the potential distribution. The highest Emesh value for Mladost Substation has been found on line 2 at the corner mesh (Fig. D2). A greater mesh voltage could be expected at mesh P, being again of no actual significance. The results presented in Table DI show that the approximate formulas can provide a fair assessment of mesh voltages also for slightly asymmetrical grids.

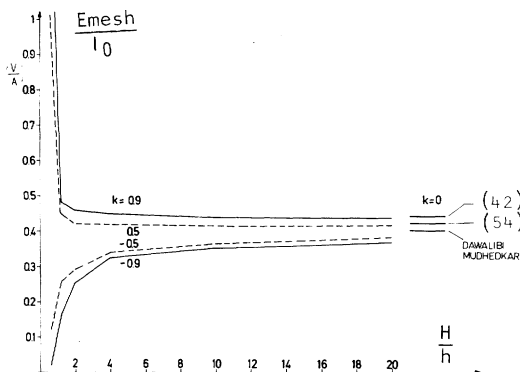


Fig. D3 Sixteen-mesh grid mesh voltages

To investigate the applicability of simplified formulas for assessing the mesh (touch) voltages in nonuniform soil, the data on a 16-mesh, 30×30 m² ground grid buried in a two-layer soil with top soil layer resistivity $\sigma_1=100$ Ω m, reported in /D1/, have been used. The grid parameters are: $h=0.5$ m and $d=0.02$ m. Fig. D3 displays the diagrams for Emesh/ I_0 values in terms of H/h , H being the depth of the top soil layer. Parameter: $k=(\sigma_2-\sigma_1)/(\sigma_2+\sigma_1)$, σ_2 denoting the bottom layer resistivity. The Emesh/ I_0 values have been approximately calculated from the percentage mesh (touch) voltages Emesh% and from the grid resistance R , both read from the corresponding diagrams in /D1/, as: $Emesh/I_0=(Emesh\%/100)R$. The mesh voltages have been also evaluated using (42) and (54) for uniform soil with $\sigma=\sigma_1$. As evident, the simplified formulas yield a fair estimate of Emesh, at all k involved, when $H/h \geq 4$. At $k=0.5$ and 0.9 this is true also for $H/h \geq 2$. The shapes of the diagrams in Fig. D3 can be explained by the fact that Emesh% and R change inversely when H/h is increasing.

We would like again to congratulate the author for the valuable contributions for ground grid design made by the paper.

REFERENCE

[D1] F. Dawalibi, and D. Mudhedkar, "Parametric analysis of grounding grids", *IEEE Transactions*, vol. PAS-98, No. 5, pp. 1659-1667, Sept./Oct. 1979.

Manuscript received February 18, 1983.

Shashi G. Patel (Georgia Power Company, Atlanta, GA): The author has done a good job in coming up with a change in existing IEEE guide-(80) formula for Emesh, making it more accurate and sacrificing little in its simplicity. The discussor has compared the values of Emesh resulting from equation-(42) with those using an accurate computer model for ten different grids (ranging from 6×6 meshes through 30×30 meshes) in uniform resistivity soils. The Emesh values using author's equation were within 97 percent to 115 percent of computer calculated results.

Comments on following specific points are invited from the author:

1) The major drawback in existing IEEE formula for Emesh is the assumption that "the cross connections are sufficiently distant from the plane studied to have negligible effect on current flow and potential gradients within the plane". This assumption is totally invalid for a grid with square meshes. The author has obviously continued with this assumption in developing the new K_m .

Since the author has successfully compensated for the deficiency due to this assumption by introducing an arbitrary factor,

$$\frac{1}{(2N)^2/N \sqrt{1+h/h_0}}$$

in existing IEEE formula, the Emesh values will be accurate for grids with square meshes. However the discussor feels that for grids with rectangular meshes (2.5:1 maximum length to width ratio) the equation-(42) may produce considerably higher Emesh values when compared with accurate computer values.

2) In existing guide (80), the factor K_i has been determined from the equation $(K_m \times K_i)/K_m$. The product $(K_m \times K_i)$ was determined from Koch's experimental model. The author has now changed K_m with product $(K_m \times K_i)$ still remaining the same. It seems that K_i should also be changed.

3) Equation-(39) in this paper should read

$$\frac{iL}{R_g} = \frac{K_i L_1}{R_g} + \frac{K_i K_{ij} L_2}{R_g} i ; \text{ for } L_1 + L_2 = L \text{ and } K_{ij} < 1$$

to be in line with equation-(42).

Manuscript received February 15, 1983.

J. G. Sverak: The discussors have presented many interesting comments and captivating questions. To *Mr. Patel's* discussion: According to the disclosed figures on the mesh potential calculated for his 12 grids, the differences between the values of E_m calculated by Eq. (42) and the corresponding results of computer calculations are within a -3 to +15 percent range, and the deviation is no more than plus-minus 9 percent, with about a 5 percent conservative bias. To other specific points:

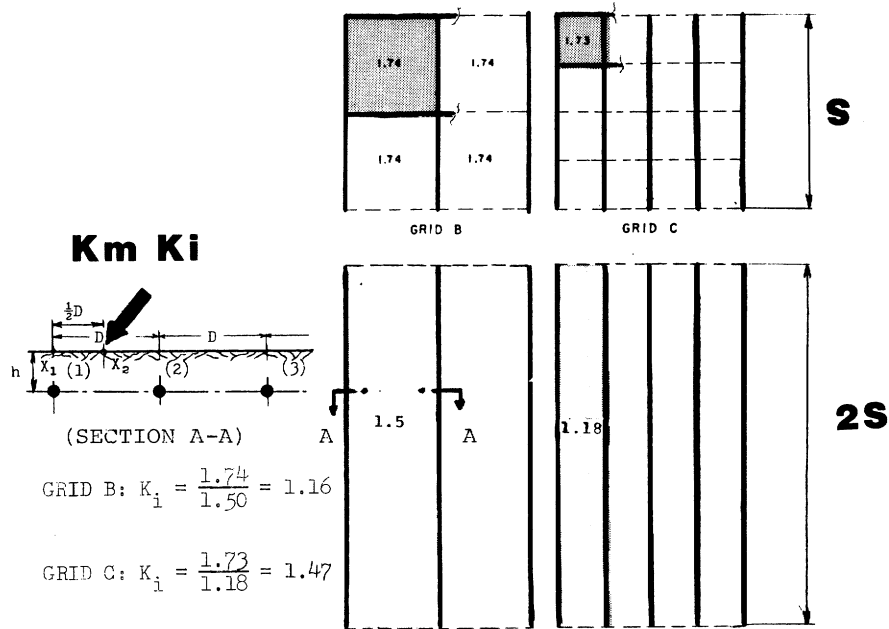


Fig. 18

1) It is somewhat of a disappointment that, after reading the paper, Mr. Patel opts to quote the old assumption about cross-connections and taking it literally for its face value, makes it the focal point of his analysis. However, a) since the combined length of all grid wires determines the value of average current density I_0/L which is used in the calculation of E_m , neither the old nor the new equations truly can - and for this matter even may - reflect such an assumption. As is obvious from Fig. 18, the basic characteristic of the IEEE model is that a single set of N parallel wires, each of length $2S$, is viewed as an acceptably close equivalent of an equally spaced square grid which consists of $2N$ wires, each of length S , covering an area $S \times S$. But, if the conductors have the same spacing as those in the grid and each dissipates current $i = I_0/L$ per unit of its length, then the size of grounding area is twice that of the grid and the number and length of conductors per unit of area is considerably reduced. Furthermore, since the cross-connections become extensions of the remaining N wires, only a half of the mutual wire-to-wire effects is eliminated, as dictated by the geometry of the incomplete model chosen. And, b) not the expression shown by the discussor (representing the product of H_m and K_{ii}), but the factor K_i compensates for the distortions due to different geometries of a grid and of the IEEE model.

However, it is difficult to understand why Mr. Patel prefers to label the product of factors K_{ii} and H_m as "arbitrary". Although K_{ii} and H_m roles are different from what he assumes, there is nothing arbitrary about either of them. To clarify these matters, consider what is hidden behind the words "irregularity factor" and what is and has always been the true purpose of K_i , and what is accomplished by K_{ii} and H_m .

Role of K_i . Because the conductor-to-conductor geometry of a grid is clearly a two-coordinate affair which in terms of the model is reduced into that of one coordinate, the role of K_i is to compensate for this "quadratic-into-linear" degradation. Hence, K_i is defined in a form $y = C_1x + C_2$; C_1, C_2 const. is natural for such a purpose. That's what has been meant by "the straight-line function of K_i is consistent with the model used", stated in the paper. The particular form of K_i , equation (3), where $x = N$, $C_1 = 0.172$, and $C_2 = 0.656$, can be easily traced down: as it has already become apparent from Figure 18, K_i was devised to match the K_m values calculated on the basis of N wire model, to the corresponding true values of K_m which were extracted from Koch's experimental data. There is nothing wrong with this approach; a simple formula does not mean that the approach is simplistic. And, furthermore, the linear form of K_i has one undeniably good quality: It does not add any hard-to-control problems of its own to the calculated product, E_m . That to tame a non-linear K_i can be a hand full, is documented in the discussion of ref. [28] by this author, with which Mr. Patel is certainly familiar. He is right, however, in suggesting that for (square) grids with rectangular meshes or, more importantly, for equally spaced rectangular grids with square meshes, equation (42) will tend to produce rather high E_m values. Yet, this will occur only if the grid has more parallel wires in one direction (N_a) than in the other one (N_b), and if N is taken as the maximum of the two counts. Because

of the already explained role of K_i , in such a case, say for a $50m \times 150m$ grid with 9 subdivisions along one side ($N_a = 10$) and 27 subdivisions along the other side ($N_b = 28$), the geometric mean of the two values ought to be used as an equivalent value of N ; $N = \sqrt{28 \times 10} \approx 17$. It is indeed fortunate that the discussor has focused on this important aspect of determining N for a rectangular grid, which is not mentioned in the paper.

Role of K_{ii} . Because K_i corrects only for the grid geometry, another corrective factor is needed to account for the fact the a superposition of the individual current contributions, wire by wire, neglects that distortions of the gradient field must simultaneously occur due to the presence of other wires. K_{ii} is meant to fill this need. In other words, if the corner mesh voltage is expressed in the canonical form of (12), as $E_{mj} = |rij| |ik|$, then K_i reflects the shortage of $|rij|$ terms, while K_{ii} accounts for the effect of $|ik|$ terms which influence the gradient field near the point on the ground surface above the corner mesh, where E_m is to be determined.

Eq. (42): The assumption is that with increasing N , the resulting relative increase of the electrically "flat" inner area of the grid and of the number of conductor segments carrying lower current, somewhat reduces the overall effect of $N - 2$ outside wires on diminishing the "corner mesh" voltage between the first two wires of the subject N wire model. However, no exact science can be claimed where none is possible. For instance, it is next to impossible to decide whether such an effect will tend to be more prominent with increasing N or not. As determined experimentally, it appears that in terms of this very imperfect model, the relative increase of the current magnitude in the wires near the peripheral ones, outweighs the overall impact of a greater number of inner wires carrying much lower current. But the observation may well be just unique to this specific IEEE model. No matter what, Fig. 19 gives a reasonable idea as to how the resulting semi-empirical factor K_{ii} modifies the K_i curve for $N-2$ outside wires.

Eq. (41): The basic idea of setting $K_{ii} = 1$ is, perhaps surprisingly, more artificial: By neglecting the need to compensate, the beneficial effect of $N-2$ inner wires upon lowering E_m is increased. The increase "accounts" for the presence of peripheral ground rods which are known to decrease the magnitude of currents flowing in the peripheral wires ($N = 1, 2$) more, and the magnitude of currents in the other conductors closer to the center of a grid less.

Role of H_m . Several disadvantages result from using Koch's grids as a reference. These models are not scale-down design of practical grids; each model grid was made of a copper wire 0.2 mm (0.0002 m) in diameter, and each grid pattern arranged in a 120 mm x 120 mm square. If a copper conductor of 2/0 AWG size is considered as typical for small substation grids, $d = 10.5$ mm. Consequently for a 64 mesh grid, the actual size of Koch's model would be $S = 0.12$ m x $(10.5 / 0.2) = 6.3$ m and the spacing and depth would be $D = 0.79$ m and $h = 0.005$ m, respectively. In his paper, Koch gave $S = 13.8$ m, which

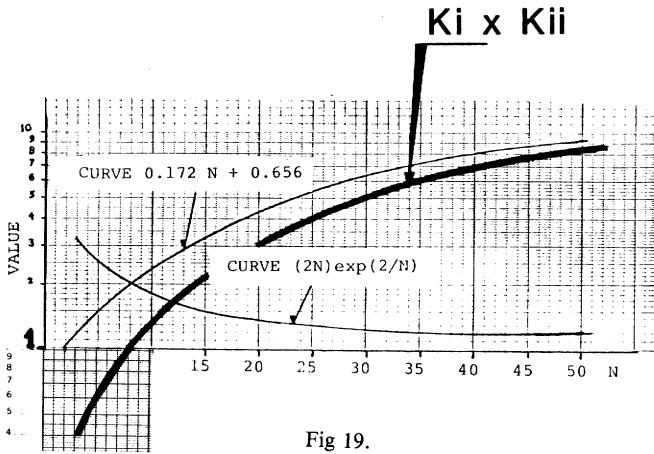


Fig 19.

was based on the dimension of a 30 mm x 3 mm ground strap. Since not the cross-section but the circumference of a conductor determines its performance, per unit of length, in discharging current into the ground, the paper indicated $d = 23$ mm as an equivalent diameter of the ground strap. However, regardless of the scaling ratio, the depth of grid burial h remains near-zero.

Table III presents re-calculation of the Koch's models for $h = 0.1$ mm, the grid patterns A($N=2$), B($n=3$), C($N=5$), D($N=9$), and continuing additional subdivisions up to $N=30$. Furthermore, in order to illustrate the behavior of the old equations if larger depths are used, two more columns are printed for h increased to 0.5 mm and 1.0 mm. Resulting products of $K_i \times K_m$ are shown as follows.

In Table III, column |I| is calculated by equation (18), column |II| by (19-21), and column |III| by (I-20), respectively. As indicated, for $h = 0.1$ mm there is not the slightest hint that the equations can become negative or that for larger values of h - because of the lack of this parameter in $N-2$ terms and the asymmetrical condition of the first two wires - the simplified formula (18) will tend to become negative

more rapidly; here for $h = 0.5$ mm at $N = 24$, and for $h = 1$ mm at $N = 19$, as opposed to $N = 25$ and $N = 21$ for the other equations. The role of H_m is to compensate for the former, while a better simplification of K_m for the first two wires corrects the latter problem; eq. (35).

2) One also finds it hard to share the idea that K_i should be changed because K_m is now defined by a different formula. Most shortcomings of the old formula resulted from a certain misconception as to how far the results of Koch's experiment - which he had done with small square grids submerged just under the water's surface—can or may be extrapolated by simple analytical means, in order to make them applicable to large rectangular grids buried in a shallow but decidedly non-zero depth. In this context, the new formulas (41,42) simply offer a bit more refined approach to this goal. There is nothing sacred about the old K_m . It was good for just what it had been derived from: A square grid having no more than 64 meshes, not too densely spaced, and buried very close to the ground surface. As long as $h \ll D$, and $N < 10$, there is minimum difference in K_m values calculated by either formula. When a wider range of parameters is allowed, the new simplified equations remain "faithful" to the premises of the basic mathematical model over a far larger part of the entire parameter range than the old ones. Thus, in spite of the changes, Eqs. (41, 42) work well with K_i as is.

3) The suggested formulation of Eq. (39) probably is more consistent with that of Eq. (42), though the improvement is rather academic. In fact, the only purpose of Eq. (39) is to symbolize that if an increase of the current density occurs in some part of a grounding grid, and the value of current I_0 injected into the grid remains unchanged, then there has to be a corresponding decrease of the current density in other parts. Naturally, if the former is realized by means of a multiplier $K_i > 1$, then it is logical to use a second corrective factor $K_{ii} < 1$, to reduce the relative magnitude of current $i = I_0/L$, in p.u. of conductor length, in the rest of the grid. But, of course, it does not generally follow from (39) that numerically the condition $L = K_i L_1 + K_{ii} L_2$, or in the case of Mr. Patel's version of (39), $L = K_i L_1 + K_i K_{ii} L_2$, must hold true for $L = L_1 + L_2$.

Appreciating Mr. Patel's contribution, it appears that the brevity of Appendix II makes it difficult to recognize that the first part of K_m in formula (35) is a fully legitimate simplification of the principal model of two peripheral conductors per equation (II-10). Since a few related questions to the origins of equation (II-7) were presented by others oral-

Ki Km SERIES FOR KOCH'S GRIDS

SUBDIV.	N	D	1 x h			5 x h			10 x h		
			I	II	III	I	II	III	I	II	III
2	120.00		1.71	1.82	1.82	1.45	1.47	1.47	1.34	1.35	1.35
3	60.00		1.63	1.76	1.76	1.33	1.35	1.35	1.20	1.21	1.21
4	40.00		1.62	1.77	1.77	1.28	1.30	1.30	1.13	1.14	1.14
5	30.00		1.62	1.79	1.79	1.24	1.26	1.26	1.07	1.08	1.08
6	24.00		1.63	1.82	1.82	1.20	1.23	1.23	1.01	1.03	1.03
7	20.00		1.64	1.84	1.84	1.16	1.20	1.20	0.96	0.98	0.98
8	17.14		1.64	1.87	1.87	1.12	1.16	1.16	0.90	0.92	0.92
9	15.00		1.64	1.89	1.89	1.08	1.12	1.12	0.84	0.87	0.86
10	13.33		1.64	1.90	1.90	1.03	1.07	1.07	0.77	0.80	0.80
11	12.00		1.63	1.91	1.91	0.98	1.03	1.03	0.70	0.74	0.74
12	10.91		1.62	1.92	1.92	0.92	0.97	0.97	0.62	0.67	0.67
13	10.00		1.60	1.92	1.92	0.86	0.92	0.92	0.54	0.60	0.59
14	9.23		1.58	1.92	1.92	0.80	0.86	0.86	0.46	0.52	0.52
15	8.57		1.56	1.91	1.91	0.73	0.79	0.79	0.37	0.45	0.44
16	8.00		1.53	1.90	1.90	0.65	0.73	0.72	0.28	0.37	0.36
17	7.50		1.49	1.89	1.89	0.58	0.66	0.65	0.18	0.28	0.27
18	7.06		1.46	1.87	1.87	0.50	0.58	0.58	0.08	0.20	0.18
19	6.67		1.42	1.85	1.85	0.41	0.50	0.50	-0.02	0.11	0.09
20	6.32		1.38	1.83	1.83	0.33	0.42	0.42	-0.13	0.02	0.00
21	6.00		1.33	1.80	1.80	0.24	0.34	0.34	-0.26	-0.07	-0.09
22	5.71		1.28	1.77	1.77	0.14	0.26	0.25	-0.35	-0.11	-0.13
23	5.45		1.23	1.74	1.74	0.05	0.17	0.16	-0.46	-0.26	-0.28
24	5.22		1.17	1.70	1.70	-0.02	0.08	0.07	-0.58	-0.35	-0.38
25	5.00		1.11	1.66	1.66	-0.16	-0.02	-0.02	-0.70	-0.45	-0.49
26	4.80		1.05	1.62	1.62	-0.26	-0.11	-0.12	-0.83	-0.55	-0.58
27	4.62		0.99	1.58	1.58	-0.37	-0.21	-0.22	-0.95	-0.65	-0.69
28	4.44		0.92	1.53	1.53	-0.48	-0.31	-0.32	-1.08	-0.75	-0.80
29	4.29		0.85	1.48	1.48	-0.59	-0.41	-0.42	-1.21	-0.85	-0.91
30	4.14		0.78	1.43	1.43	-0.71	-0.51	-0.52	-1.35	-0.95	-1.01

N =	2	3	5	9	n/a	n/a
GRID	A	B	C	D	E	F
MAXIMUM VALUE $K_m \times K_i$ RECORDED	1.83	1.74	1.73	1.90	2.23	2.23
COEFFICIENT K_m COMPUTED	1.82	1.50	1.18	0.86	1.50	1.50
COEFF. $K_i = \frac{K_m \times K_i}{K_m}$	1.00	1.16	1.47	2.21	1.49	1.49

TABLE III.

ly, a detail simplification process leading to (II-7) and, consequently to (II-10), is presented below.

First, neglecting d in (II-5) and using a square of (II-3), the obtained two equations are added by a multiplication of arguments under the logarithm:

$$\begin{aligned} K_{mx}(2) + K_{my}(2) &= \frac{1}{4\pi} \ln \left[\frac{(4h^2 + D^2)(4h^2 + D^2)(h^2 + D^2)}{(4h^2 + 4D^2)(4h^2 + 4D^2)(D^2 + 0)} \frac{(h^2 + D^2)}{D^2 + (2h - 0)^2} \right] = \\ &= \frac{1}{4\pi} \ln \left[\frac{(4h^2 + D^2)^2}{16(h^2 + D^2)^2} \frac{(h^2 + D^2)^2}{D^2(D^2 + 4h^2)} \right] = \frac{1}{4\pi} \ln \left[\frac{4h^2 + D^2}{16D^2} \right] = \\ &= \frac{1}{4\pi} \ln \left[\frac{h^2}{4D^2} + \frac{1}{16} \right] = \frac{1}{4\pi} \ln \left[(h/2D)^2 + \left(\frac{1}{4}\right)^2 \right] \quad (\text{II-7a}) \end{aligned}$$

Next, the following deliberate simplification can be made:

$$\frac{1}{4\pi} \ln \left[(h/2D)^2 + \left(\frac{1}{4}\right)^2 \right] \approx \frac{1}{2\pi} \ln \left[(h/2D) + \left(\frac{1}{4}\right) \right] \quad (\text{II-7b})$$

Of course, a detail analysis of (II-7b) reveals that

$$\frac{h^2}{4D^2} + \frac{1}{16} \neq \frac{h}{4D} + \frac{1}{4D} + \frac{1}{16},$$

because an extra term $h/4D$ is present in the simplified equation (II-7), shown here on the right side of (II-7b). This added term plays a very useful role: For small values of h and large D 's it is negligible, while for dense spacings and the depth h approaching D , it slightly increases the combined value of the argument under the logarithm. This effect tends to rectify the conceptual deficiency of the basic mathematical model in this respect. Hence, Eq. (II-7) can be viewed as a simplified equation with a correctly applied error bias.

Dr. Nahman's comments and the data he provides, are very valuable. For instance, his results for a metal plate are indeed of interest, because these provide a true reference to Tables I and II. In the comparative series produced by the computer, the condition of a "solid plate" was actually obtained by setting $D = d$ in the algorithm. Hence, for the given 40 m x 40 m grid area and the conductor diameter $d = 10$ mm, the last result was for $N = 40/0.01 = 4000$, i.e. the plate was simulated as a dense "grid" consisting of 4000 parallel conductors touching each other, side by side.

The two given examples of a grid design used in the 400 kV stations Mladost and Titograd, well illustrate the usual dilemma facing anyone who wants to utilize simplified equations for a specific design that does not agree with the idealized assumptions upon which the equations are based: Can one use the equations, and if so, then how? Here, in both cases, the application of equation (41) or (42) would entail the following steps:

- Step 1 Define an equivalent rectangular grid having the same area as the grid under consideration.
- Step 2 Establish the nearest effective conductor pattern (which may differ from the actual pattern of grid conductors upon which the estimate of a total buried length will be based), and determine the equivalent value of N as a geometric mean of the number of parallel wires in each direction for the effective pattern.
- Step 3 Using the value of N from step 2, proceed with the calculation, but estimate the total buried length of ground conductors from the actual design data.

Applying this procedure to the grid design of Fig. D2 (Substation Mladost), one gets:

1) equivalent rectangular grid area 153 m x 444 m; 2) effective conductor pattern for an equally spaced grid 7 x 18, and $N = \sqrt{126} \approx 11$; 3) Assuming that no ground rods are used, L per Figure D2, is $L = 11 \times 444 \text{ m} + 11 \times 132 \text{ m} + 8 \times 173 \text{ m} = 7,720 \text{ m}$. Finally, using (42) for $h = 0.7 \text{ m}$, $d = 0.01 \text{ m}$, $\delta = 100 \text{ ohm-m}$, and $I_0 = 10,000 \text{ A}$, and entering $K_i(N=11) = 2.55$, $K_{ii}(N=11) = 0.57$, $K_h(h=0.7) = 0.767$, and $D = \sqrt{(153 \text{ m} \times 444 \text{ m}) / (11-1)} \approx 26 \text{ m}$.

$$\begin{aligned} E_m &= 100 \frac{10,000}{7,720} \frac{2.55}{2\pi} \left[\ln(6,035.7 + 360.94 - 17.5) \right. \\ &\quad \left. - 0.767 \ln(0.121) 0.57 \right] = \\ &= 52.57 \left[8.7608 - 0.9233 \right] = \underline{412.02 \text{ volts}} . \end{aligned}$$

The family of curves for a sixteen mesh grid shown in Fig. D3 very much confirms similar observations made by this author. The inclusion of parameter k is most welcome, as some aspects of using the simplified method for the case of a two-layer soil environment will be exploited in Part II of this paper.

Responding to *Mr. Rogers's* comments: Although equation (41) has been checked against the known results for a number of typical grid-rod arrangements, no detail analysis of the relationship between a rod length, number of rods and the grid size, has been done. However, an additional insight into these matters and as to how much of an effect the perimeter rods have on the value of external touch and step voltages, will be provided in Part II (written jointly with R. J. Heppel), subtitled "A Tandem Approach to Approximate and Exact Computer Solutions for Progressively Spaced Grids With Ground Rods".

Mr. Rogers is right in pointing out the significance of soil resistivity variations and, in the case of non-uniform soils, of the pronounced effect of deeper soils. Also this subject will be addressed in Part II.

As to what concerns the determination of H_m , and the development and testing of Eqs. (41, 42): After Eqs. (II-10) and (III-17) had been determined analytically, an acceptably simple expression for the corrective factor $H_m(h, h_0)$ was found by experimenting with several semi-empirical expressions, by trying to balance the left and right sides of Eq. (32) over a wide range of h , D and N . Next, with (41) assembled and K_{ii} set equal to one, examples from the literature were used to ascertain the applicability of Eq. (41) for ground rods, and later to "tune-up" K_{ii} for its final application in (42) for grids without rods or with rods evenly spread over the grid area, while retaining Eq. (41) for the case of peripheral rods. Thereafter, the equations have been submitted to the Substation Committee Working Group 78.1 for further testing. The test set of twelve square grids mentioned by *Mr. Patel* has been developed by him for this purpose. In addition to Eqs. (41) and (42), also Eq. (45) for the grid resistance and a new formula for calculating step potentials if the depth h is greater than 0.25 m, have also been included in the test. The new formula, Eq. (69) below, utilizes a faster decreasing geometric series in comparison to the old IEEE formula for E_{step} :

$$\begin{aligned} E_{step} &= \sigma \frac{I}{\pi} \left[\frac{1}{2h} + \frac{1}{D+h} + \frac{1}{2D} + \frac{1}{4D} + \dots + \frac{1}{(2)^{N-1}D} \right] K_i \\ &= \sigma \frac{I}{\pi L} K_i \left[\frac{1}{2h} + \frac{1}{D+h} + \frac{1}{D} \left[1 - \left(\frac{1}{2}\right)^{N-2} \right] \right] \quad (69) \end{aligned}$$

Consequently, all these new equations developed by this author, i.e. Eqs. (41), (42), (45) and (69), have been tested against the results of computer calculations done at the Georgia Institute of Technology in the framework of project RP 1494-2, sponsored by EPRI. The validity of the computer algorithm used there has been justified on the basis of comparison of certain results to the outcome of a scale model experiment in electrolytic tank, done at the Ohio State University as part of RP 1494-3. Furthermore, some additional comparisons for rectangular grids are shown in the discussion part of /27/. And last, but not least several grid configurations have been verified with the use of Heppel's algorithm, described in /17/. For instance, for a 16 x 16 conductor pattern and $h = 0.5 \text{ m}$, with other grid data being identical to those used for Tables I and II, Eq. (42) gives $E_m = 152.9 \text{ volts}$, while Heppel's algorithm yields $E_m = 146 \text{ volts}$. However, as shown in Fig. 20, if standing exactly above the corner of such a grid, one would be subjected to a much higher potential of 191 volts! Therefore, in a way, this last result confirms the correctness of two early theoretical concepts around which the development of program RENA evolved /7/, and which will be further exploited in Part II of this paper: (1) the envelope of the earth surface potential curves is distinctly convex for ground grids with many meshes, and (2) partly because of 1, and partly for both practical and analytical reasons, it is more logical to pursue the development of approximate methods which can yield a near-optimal pattern of progressively spaced grid conductors than to struggle with an over-constrained problem which - if no ground rods are assumed - may eventually yield an impractical answer.

271	238	198	148	100	88	85	77	64	49*	48	55	57	52	43
275	242	202	153	108	100	98	90	77	61*	58	65	66	62	52
280	246	206	157	112	105	103	96	82	66*	63	69	71	66	57
285	251	210	159	112	103	101	93	79	63*	61	68	69	65	55
291	256	214	160	107	94	91	83	69	53*	52	61	63	58	48
297	263	220	164	108	95	93	85	70	52*	53	63	66	61	49
305	271	228	173	120	113	114	106	91	70*	69	79	82	77	64
315	281	239	184	134	129	130	122	106	85*	83	93	96	90	77
326	293	252	198	147	139	139	130	114	93*	91	101	103	98	85
339	308	269	217	162	146	139	129	113	95*	94	103	105	100	88
353	325	291	245	191**	162**	147**	134**	120**	108**	107**	112**	112**	108**	100**
368	344	316	282	245	217	198	184	173	164	160	159	157	153	148
383	363	340	316	291	269	252	239	228	220	214	210	206	202	198

FIG. 20.

With regard to the question of using H_m , to improve eq. (67) of reference [2]: because of the result of calculations done in paragraph 4.5 with the use of eq. (34), it is felt that such a refinement is not worthwhile. But if a better accuracy of the basic mathematical model is what Mr. Rogers has had in mind, it is possible to upgrade the nonsimplified formula for K_m to a level which is consistent with that of Eq's (41) and (42). Since the resulting formula will most likely be use in computer applications, a suitable algorithm in Fortran is provided below; Fig. 21.

```

PI=2.*ASIN(1.)
CALL FULNEW(CMF,2,CDIA,DPTH,SPAC,NC,2,PI)
SUBROUTINE FULNEW(CKM,KEY,CDIA,DPTH,SPAC,NX,NY,PI)
C
TERM(A,B,C,D)=(A*A+B*B)/(C*C+D*D)
RA=CDIA/2.
RB=2.*DPTH-RA
DO 7 I=1,2
GOTO(1,2),I
1 N1=1
N2=2
GOTO 3
2 N1=3
N2=NX
3 I1=1.
I2=1.
T3=1.
DO 4 M=N1,N2
DK=SPAC*FLOAT(M-1)
DM=SPAC*FLOAT(2*M-3)/2.
T1=11*TERM(DPTH,DM,DPTH,DK)
IF(M.GT.NY)GOTO 4
T2=T2*TERM(DPTH,DK,RA,DK)
T3=13*TERM(DPTH,DK,RB,DK)
4 CONTINUE
GOTO(5,6),I
5 EX2=2.*ALOG(T1)
EY2=ALOG(T2)+ALOG(T3)
GOTO 7
6 CII=1.
IF(KEY.EQ.2)CII=FLOAT(2*NX)**(-2./NX)
EXF=EX2+CII*2.*ALOG(T1)/SORT(1.+DPTH)
EYF=EY2+CII*(ALOG(T2)+ALOG(T3))
GOTO 8
7 CONTINUE
8 CKM=(EXF+EYF)/(4.*PI)
9 RETURN
END

```

Fig. 21.

FULNEW above represents a modified version of subroutine FULSER, described in paragraph 5.2, which now includes both K_{ii} and $H_m(ho, h)$. This routine allows the following choices in calculating K_m for a N conductor set:

a) By entering "1" as the value of "KEY" in the calling statement and using "2" for "NY" (number of calculated Ey components), the value of K_m , which is returned as "CKM", corresponds to the condition of ground rods placed predominantly along a grid perimeter, Eq. (41).

b) Entering "2" for "KEY" and again using "2" for "NY" yields K_m which is consistent with the conditions of Eq. (42), i.e. no ground rods, or ground rods evenly spread over the grid area.

Furthermore, by increasing the number of Ey terms calculated per (b), i.e. using a value between 3 and N for "NY", one can achieve a certain moderating effect which for the ultimate value of "NY" being the same as "NX" (i.e. $NX = NY = N$), will produce a result about half-way between the results for (a) and (b) conditions. This may be used for differentiating between various grid-rod patterns. Finally, by setting "NY" equal to "1", and "KEY" to "2", one would get a "refined" asymmetrical model corresponding to the old formula (69) of the Guide, mentioned by Mr. Rogers.

N	D	EM-1	EM-3	EM-4	EMNEWO	EM1-N	EMZUK	EMZIN	EMNAH	EMNEW1	EMNEW2	RGNEW	RCNAH	RGSHWZ	RGGET	EM exact
AREA (M X M)	SOIL (OHM-M)	H (M)	DIAM. (MM)	CURRENT (A)	PATTERN N X N	STEPFULL	STEPSIMPL	STEPNEW								
10.97 X 10.97	170.000	0.610	13.259	860.700	17 X 17	964.05	907.76	872.93	7 VOLTS							803.0
7	1.8	411.9	576.9	545.4	801.6	746.6	402.2	1046.5	1053.4							
AREA (M X M)	SOIL (OHM-M)	H (M)	DIAM. (MM)	CURRENT (A)	PATTERN N X N	STEPFULL	STEPSIMPL	STEPNEW								
17.98 X 17.98	150.000	0.457	10.998	1404.400	11 X 11	1093.61	1109.37	991.30	7 VOLTS							669.0
11	1.8	346.3	437.1	418.9	661.2	1301.3	343.5	735.6	942.2							
AREA (M X M)	SOIL (OHM-M)	H (M)	DIAM. (MM)	CURRENT (A)	PATTERN N X N	STEPFULL	STEPSIMPL	STEPNEW								
27.43 X 27.43	150.000	0.610	13.259	1993.000	16 X 16	886.13	907.76	655.37	7 VOLTS							587.5
16	1.8	141.9	264.8	219.6	471.7	1316.2	147.3	455.8	790.7							
AREA (M X M)	SOIL (OHM-M)	H (M)	DIAM. (MM)	CURRENT (A)	PATTERN N X N	STEPFULL	STEPSIMPL	STEPNEW								
45.11 X 45.11	1400.000	0.500	16.998	1423.000	16 X 16	2162.58	2171.33	1727.06	7 VOLTS							1782.0
14	3.0	1388.8	1492.2	1470.6	2100.6	6098.8	1384.8	1865.8	2436.4							
AREA (M X M)	SOIL (OHM-M)	H (M)	DIAM. (MM)	CURRENT (A)	PATTERN N X N	STEPFULL	STEPSIMPL	STEPNEW								
39.01 X 39.01	150.000	0.457	10.516	2941.000	17 X 17	897.83	908.12	699.58	7 VOLTS							654.0
17	2.4	310.7	386.9	377.4	598.5	2163.9	343.1	564.5	844.4							
AREA (M X M)	SOIL (OHM-M)	H (M)	DIAM. (MM)	CURRENT (A)	PATTERN N X N	STEPFULL	STEPSIMPL	STEPNEW								
44.77 X 44.77	150.000	0.610	10.516	3671.000	17 X 17	694.69	700.52	517.12	7 VOLTS							671.5
17	3.0	370.2	421.8	411.0	644.9	1873.2	372.0	580.6	855.5							
AREA (M X M)	SOIL (OHM-M)	H (M)	DIAM. (MM)	CURRENT (A)	PATTERN N X N	STEPFULL	STEPSIMPL	STEPNEW								
60.05 X 60.05	150.000	0.457	10.998	4590.000	21 X 21	821.91	826.40	615.46	7 VOLTS							619.0
21	3.0	361.5	392.5	386.1	603.1	2405.3	366.2	531.9	839.2							
AREA (M X M)	SOIL (OHM-M)	H (M)	DIAM. (MM)	CURRENT (A)	PATTERN N X N	STEPFULL	STEPSIMPL	STEPNEW								
60.05 X 60.05	150.000	0.457	9.997	10000.000	21 X 21	1790.64	1800.43	1384.46	7 VOLTS							1275.0
21	3.0	426.1	493.3	479.5	1352.2	5496.3	835.4	1180.9	1828.1							
AREA (M X M)	SOIL (OHM-M)	H (M)	DIAM. (MM)	CURRENT (A)	PATTERN N X N	STEPFULL	STEPSIMPL	STEPNEW								
121.92 X 121.92	150.000	0.610	10.516	9001.000	21 X 21	495.78	496.23	405.41	7 VOLTS							739.0
21	6.1	559.1	572.6	569.9	792.3	1339.4	558.9	634.6	882.2							
AREA (M X M)	SOIL (OHM-M)	H (M)	DIAM. (MM)	CURRENT (A)	PATTERN N X N	STEPFULL	STEPSIMPL	STEPNEW								
78.03 X 78.03	150.000	0.457	9.997	10000.000	27 X 27	1382.48	1392.40	1029.41	7 VOLTS							911.0
27	3.0	536.1	586.1	575.7	927.2	4903.3	550.7	774.2	1344.5							
AREA (M X M)	SOIL (OHM-M)	H (M)	DIAM. (MM)	CURRENT (A)	PATTERN N X N	STEPFULL	STEPSIMPL	STEPNEW								
137.16 X 137.16	150.000	0.610	10.516	10293.000	31 X 31	570.82	574.21	425.80	7 VOLTS							609.0
31	4.6	371.5	393.8	389.2	607.5	2388.7	380.3	467.7	806.3							
AREA (M X M)	SOIL (OHM-M)	H (M)	DIAM. (MM)	CURRENT (A)	PATTERN N X N	STEPFULL	STEPSIMPL	STEPNEW								
273.10 X 273.10	150.000	0.457	10.998	20320.004	31 X 31	522.33	522.21	448.36	7 VOLTS							696.0
31	9.1	646.0	650.2	649.5	848.0	1573.1	647.8	629.2	905.3							

TABLE IV.

Table IV above shows in column EMNEWO the results obtained with FULNEW for condition (b), and the corresponding results of using Eq. (41), column EMNEW1, and of Eq. (42), column EMNEW2, for the particular test data of twelve square grids discussed by Mr. Patel. In addition to the symbols already explained, or defined in paragraph 5.5, here

- EM EXACT is mesh voltage calculated by a computer algorithm of EPRI RP-1494-2, ref. /28/, in volts;
- RGSHWZ is grid resistance calculated by Schwarz /22/, in ohms;
- RGGET is grid resistance by a simplified set of tabulated factors of ref. /28/, in ohms;
- STEPFULL is step voltage calculated by formula (50) of Appendix I of Guide 80, in volts;
- STEPSIMPL is step voltage calculated by simplified formula (22) of Guide 80, in volts;
- STEPNEW is step voltage by a new formula for depth $h > 0.25$ m, Eq. (69), in volts.

Mr. Jackson is correct in observing that Eq. (59) cannot hold for a thin top layer of crushed rock, if $0 < h' < 3a$. Actually, the main purpose of paragraph 7.3. is tutorial. Since a set of derating curves for C, with C defined as

$$C = \frac{1}{0.96} \left[1 + 2 \sum_{\xi=1}^{\infty} \frac{k^{\xi}}{\sqrt{1 + (25\xi h')^2}} \right] \quad (70)$$

where

$$k = (p - p_0) / (p + p_0)$$

has been available in /26/, the whole idea of using the hemisphere concept in this paper, is to illuminate the problem from a different angle and, with the use of simplest analytical expressions, to

- demonstrate the validity of the derating principle in general, and
- call attention to the fact that for dense grids with many conductors in shallow depth, the seemingly too simple approach used in the previous editions of Guide 80, i.e. the assumption of an infinitely thick top layer, has not been such a bad idea, after all!

The uncertainty about the sign of "a" in the denominator of (59) is rooted in the fact that both a hemisphere imbedded in the ground surface and a half-submerged sphere have the same resistance. As shown below, if "a" is set equal to 0.053 m (in correspondence to $r = 8$ cm for an equivalent single foot disc, upon which Eq. (70) is based), it seems that, perhaps, taking "a" out from the denominator would be the best choice with respect to Eq. (70). Comparison of the results for all three

simplified alternatives and for "C" calculated by Eq. (70), using the summation of the first 100 terms of its infinite series, is shown in Table V.

h' (M)	C PER (70)	C PER (59)	C (DWJ)	$1-a/2h'$
0.053	0.228	-0.000	0.667	0.500
0.079	0.403	0.500	0.750	0.667
0.106	0.524	0.667	0.800	0.750
0.132	0.608	0.750	0.833	0.800
0.265	0.795	0.889	0.909	0.900
0.530	0.897	0.947	0.952	0.950

TABLE V.

However, considering the complexity of the expression for "C" of Eq. (70), the merit of Mr. Jackson's contribution to making the simpler hemisphere concepts more practical, is most appreciated. In any case, one then has the choice of using a modified formula (60) to derate the allowable touch voltage more - by neglecting the presence of a grid, or of using formula (66) and derate less - by taking the grid in depth h into account. Otherwise, the use of derating curves from /26/ remains the prudent choice.

In closing, this author wishes to express his complete identification with Mr. Rogers' superb appraisal of the significance of Guide 80.

REFERENCES

[27] E. B. Joy et al., "Graphical Data for Ground Grid Analysis", *IEEE Trans. Power App. and Syst.* vol. PAS-102, no. 9, Sept. 1983, pp. 3038-3048.
 [27a] J. G. Sverak, discussion of [27] above.
 [28] E. B. Joy, A. P. Melipoulos, and R. P. Webb, "Analysis Techniques for Power Substation Grounding Systems", final report on EPRI research project No. 1494-2, July 1982.
 [29] D. G. Casten and R. Caldecott, "Transmission Grounding, Task 1: Perform Scale Model Tests", final report on EPRI research project No. 1494-3, April 1982.